Geoderma 261 (2016) 204–221

Contents lists available at ScienceDirect

Geoderma

journal homepage: www.elsevier.com/locate/geoderma

Digital mapping of soil carbon in a viticultural region of Southern Brazil

Benito R. Bonfatti [a,b,c], Alfred E. Hartemink [b,*], Elvio Giasson [a], Carlos G. Tornquist [a], Kabindra Adhikari [b]

[a] Universidade Federal do Rio Grande do Sul, UFRGS, Faculdade de Agronomia, Av. Bento Gonçalves, 7712, Porto Alegre, RS 91540-000, Brazil
[b] University of Wisconsin — Madison, Department of Soil Science, FD Hole Soils Lab, 1525 Observatory Drive, Madison, WI 53706, USA
[c] CAPES Foundation, Ministry of Education of Brazil, Brasília, DF 70040-020, Brazil

ARTICLE INFO

Article history:
Received 4 March 2015
Received in revised form 21 July 2015
Accepted 23 July 2015
Available online xxxx

Keywords:
Soil carbon
Subtropical soils
Vineyard
Carbon stocks
Inceptisols
Ultisols

ABSTRACT

There is a need for soil C assessment in the soils of tropical and subtropical areas. We have aimed to quantify the spatial extent of SOC concentration and stocks under different land use and soil types in an 8118 ha area in southern Brazil. Common soils are Inceptisols, Ultisols and Mollisols, and the dominant land use is forest and vineyard. SOC data were modeled by 5 depths deriving values from spline functions. Regression kriging was used to model SOC concentration for each depth to 100 cm, and for producing a soil depth map. Uncertainty was estimated by empirical approach, using sequential Gaussian geostatistical simulation of the residuals. The Projected Natural Vegetation Soil Carbon (PNVSC) approach was used to evaluate changes in soil carbon due to land use change. Bulk density was estimated by pedotransfer functions. SOC stocks were calculated using the SOC prediction, bulk density and the soil depth map, and the stocks were corrected by cumulative mass coordinates. The models for SOC concentration prediction explained about 44% of the variance at 30–60 cm depth and with slightly lower values for other depths. Important covariates for prediction were Soil Order (Entisols), coordinate *X*, Aspect and the DEM. The model for the prediction of soil depth explained 43% of variance and important covariates were Soil Order (Entisol, Mollisol, Ultisol), Valley Depth and TWI. Soils under forest accumulated more carbon in the top 30 cm whereas soils under pasture had higher SOC levels with depth. Soils under arable crops and vineyard had the lowest SOC concentration. SOC concentration decreases by depth, as well as prediction intervals of uncertainty, until 60 cm depth. The SOC stocks (0–100 cm) varied between 104 t C/ha in vineyards on Alfisols, and 280 t C/ha in pasture areas on Oxisols. The PNVSC analysis showed that most soils had lost SOC compared to when they were projected to be under forest.

Published by Elsevier B.V.

1. Introduction

Assessing the amount and distribution of soil organic carbon (SOC) levels is important as it provides information about soil fertility, rates of sequestration of carbon, recovery of degraded soil, or the impact of land use changes. Mapping the SOC concentration and stocks is challenging because of the considerable variation and dynamics. Spatial and temporal SOC changes are affected by natural and anthropic factors including management practices and land use changes.

Several recent studies have predicted and mapped SOC (Adhikari et al., 2014; Padarian et al., 2012; Kirsten et al., 2015; Malone et al., 2009; Mendonça-Santos et al., 2010; Ross et al., 2013; Zhang and Shao, 2014) and the estimation is based on relation between covariates (land use, soil type, slope, aspect, etc.) and SOC levels. Different covariates were found in models to explain SOC distribution. Thompson and Kolka (2005) found that more than 71% of SOC variation could be explained by slope, aspect, curvature, topographic wetness index and overland flow distance. Wiesmeier et al. (2014) found that the most important factors to predict SOC stocks were land use, soil type, soil moisture and climate. Adhikari et al. (2014) predicting SOC concentration, at different soil depths, reported that the importance of variables differed by depth. Minasny et al. (2013) synthesized a large number of digital SOC mapping studies and concluded that different covariates could explain the variation of SOC depending on the complexity of the landscape.

The majority of SOC inventory assessments to date focused the 0–20 cm or 0–30 cm surface layers, whereas considerable amounts of SOC may be present deeper in the soil profile (Lal, 2005; Rumpel and Kögel-Knabner, 2011; Minasny et al., 2013; Boddey et al., 2010). Sisti et al. (2004) studied SOC stocks down to 100 cm depth with zero tillage and conventional tillage and found, in rotations with vetch planted as a winter green-manure crop, significantly higher soil carbon and nitrogen concentrations under zero tillage, with most of the differences occurring at 30–85 cm depth. Angers and Eriksen-Hamel (2008) showed different interpretation of SOC stocks when considering different depths, in no till and full-inversion tillage. Full-inversion tillage could accumulate more

* Corresponding author.
E-mail address: hartemink@wisc.edu (A.E. Hartemink).

http://dx.doi.org/10.1016/j.geoderma.2015.07.016
0016-7061/Published by Elsevier B.V.

carbon at the bottom of the plow layer, but the SOC does not completely offset the gain under no till in the surface horizon. The authors highlight the importance of taking into account the whole profile to understand the distribution of SOC stocks.

Land use has major impacts on SOC concentration and stocks. However, these effects are also affected by soil class and depth (Hartemink and McSweeney, 2014; Nieder and Benbi, 2008). Changes in land use impacts the SOC levels and modifies soil characteristics. Several studies explained the changes of SOC with land use change. Conant et al. (2001), reviewing 115 studies, found that conversion from native land (mostly rain forest) to pasture increased soil C content for nearly 70% of the studies. Guo and Gifford (2002), compiling 74 publications, found that SOC stocks declined after land use changed from pasture to plantation (−10%), native forest to plantation (−13%), native forest to crop (−42%), and pasture to crop (−59%). However, the SOC stocks increased when the native forest was converted to pasture (+8%), crop to pasture (+19%), crop to plantation (+18%), and crop to secondary forest (+53%). Cerri and Andreux (1990) showed that C levels after 50 years of sugarcane cultivation, in São Paulo, Brazil, were 46% of the levels under primary forest.

Although there is a considerable body of research on the digital mapping of SOC in temperate regions, few studies have been conducted in the tropical and subtropical areas. Examples include Berhongaray et al. (2013) estimating SOC stocks in Argentine Pampas, Cheng et al. (2004) predicting SOC concentration in a subtropical area in China, Vasques et al. (2010) estimating SOC stocks in a subtropical watershed in Florida. Digital soil mapping has been used in Brazil (Giasson et al., 2006; Mendonça-Santos and Santos, 2007) and examples of SOC predictions include the studies by Mendonça-Santos et al. (2010) whom used regression-kriging for evaluate the SOC stocks in Rio de Janeiro State, and de Souza et al. (2014) using regression-kriging to predict SOC and clay content in Rio Doce Basin (Minas Gerais State). There have been other studies (e.g., Cerri et al., 2007; Tornquist et al., 2009b) where ecosystem models such as Century or Rothamsed C Model were applied to estimate SOC dynamics in the upper soil layers from different areas in Brazil.

The present study aimed to analyze the distribution of soil C in the grape growing region of Vale dos Vinhedos, in Rio Grande do Sul State, Brazil. The objectives were as follows: (i) to quantify and understand the spatial variation of SOC concentration by depth through digital soil mapping, and to assess the uncertainty, (ii) to quantify and map SOC stocks, and (iii) to estimate SOC changes due to land use change.

2. Materials and methods

2.1. Study area

The study was conducted in the Vale dos Vinhedos (Vineyard Valley) which is a wine production region in northeastern Rio Grande do Sul State (Fig. 1). The study area covered 8118 ha. The climate is classified as Cfb, subtropical with a mild summer, mean annual temperatures of 17.2 °C and 1736 mm annual rainfall (EMBRAPA, 2008). The dominant lithology is effusive rocks mostly from the Mesozoic Era (IBGE, 1986). Lower sequence comprises mostly basalts and diabase dikes, whereas the upper sequence has predominantly acid effusive rocks such as rhyolite and dacites.

Average soil depth is 150 cm (range from 25 to >250 cm) and many soils are stony and rocky (average 4.5% of fragments > 20 mm in diameter). In the study area, Inceptisols cover about 44%, Ultisols 29% and Mollisols almost 15% (Fig. 2). Mollisols are mostly present at lower elevations close to valley bottoms in the northern part of the study area. Soils in the western part of the study area are mainly Argissolos (Ultisols and Alfisols), Chernossolos (Mollisols), and Neossolos (Entisols and Mollisols). The eastern part has more rugged terrain and the dominant soils are Neossolos (Entisols) and Cambissolos (Inceptisols), with association of Argissolos (Ultisols and Alfisols), Latossolos (Oxisols) and Nitossolos (Oxisols and Ultisols) (Flores et al., 2012).

Forest (44%) and vineyard (31%) are the dominant land use in the study area. Deciduous forest is the main vegetation in plateau rugged areas, and Araucaria forest in flatter areas (IBGE, 1986).

2.2. Soil and environmental data

The soil data were obtained from the soil survey project "Os Solos do Vale dos Vinhedos" (Flores et al., 2012). Sample points were selected along predefined paths representing different landscape units (Flores et al., 2012). Sampling was done with 163 total pedons, comprising 580 soil horizons. The soils were analyzed following Brazilian standard methods (Santos et al., 2006): SOC analysis by Walkley–Black wet oxidation.

Additionally, in 2014, samples were obtained from 10 pedons (34 horizons) for an estimate of soil bulk density of the Flores et al. (2012) soil survey, allocated by contrasting land uses (vineyard, forest/planted forest, pasture, arable crops, and fallow) and soil classes. The 10 measured bulk density were used to evaluate three pedotransfer functions, which were chosen based on studies that include data from subtropical

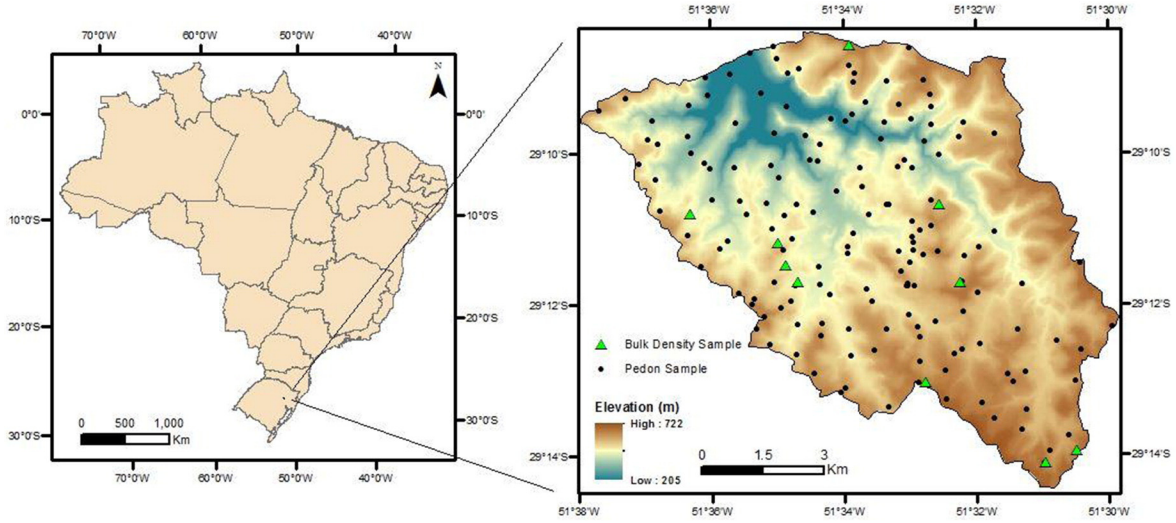

Fig. 1. Study area (Vale dos Vinhedos) in Rio Grande do Sul, Brazil (8118 ha) and location of the 163 pedons and 10 bulk density pedon sampling points.

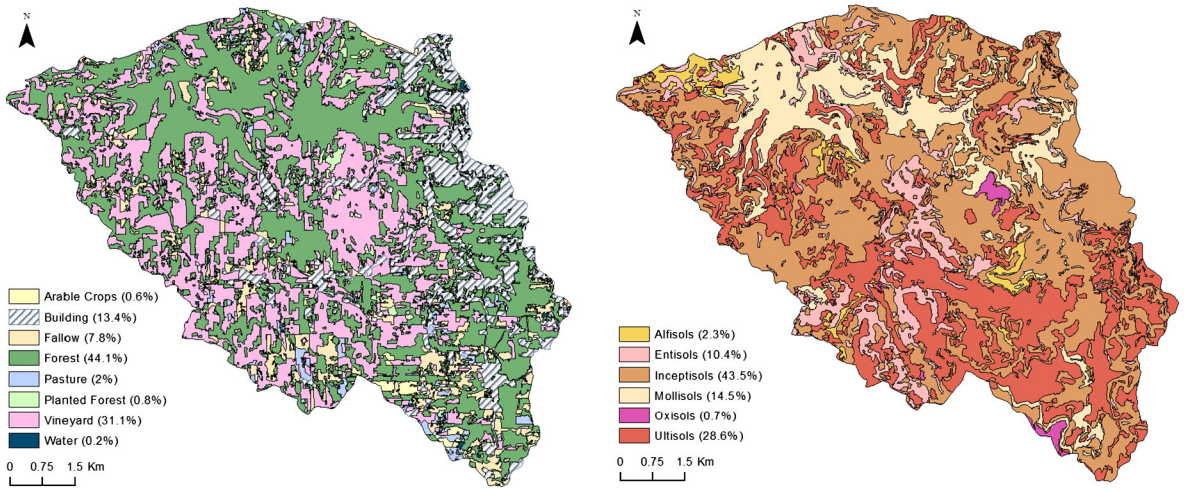

Fig. 2. Land use and soil taxonomy map of Vale dos Vinhedos in Rio Grande do Sul, Brazil. Percentages of different land use and soil order classes in parentheses.

soils. Table 1 lists measured bulk density, pedotransfer functions, and validation using root mean square error (RMSE).

Based on the lower value of RMSE (0.11), the simplified equation of Benites et al. (2007) — Eq. (2) in Table 1 — was chosen to extrapolate the bulk density for the whole dataset, producing 163 bulk density estimates. This function was developed from a large compilation of pedons from the Brazilian soil survey database maintained by EMBRAPA (Empresa Brasileira de Pesquisa Agropecuária) that include pedons in Rio Grande do Sul State (Tornquist et al., 2009a; Benites et al., 2007). Once the bulk density was calculated, the values were splined to derive bulk density for the 5 GlobalSoilMap standard depths. These values were then attributed to each map unit of Flores et al. (2012) soil map (scale 1:10.000) considering the reference soil profiles, extrapolating then to the whole study area.

On SOC concentration and soil depth predictions the following data layers from Flores et al. (2012) were used: 5 × 5 m grid resolution DEM, a soil map (scale 1:10,000) and orthorectified aerial imagery. The DEM was upscaled to 15 m grid cell size. The original soil legend of the Flores et al. (2012) survey, published according to the Brazilian soil classification (SiBCS), was converted to Soil Taxonomy (12th ed, 2014) using pedon data (clay content, pH, thickness, carbon content, texture, color, clay skins and drainage) and additional guidance from the correlation table proposed by Anjos et al. (2012).

A land use map was made using the orthorectified mosaic of aerial images from November 2005 (Flores et al., 2012). Initially, a supervised classification was performed after the images were filtered 3 times (3 × 3, 5 × 5, 7 × 7) using the mean. The supervised classification identified land uses for approximately 50% of the area particularly in the forested areas. Land use in the other half area was delimited manually. The final land use map contains 8 classes namely vineyard, forest, planted forest, pasture, arable crops, fallow, building and water bodies. Building and water bodies were masked.

A set of terrain attributes was derived from the DEM including Slope, Aspect, Valley Depth, Topographic Wetness Index, Overland Distance to Channel Network and others. A map with 13 landform classes was made in LandMapR software using the DEM (MacMillan, 2003). The covariates used for predicting the SOC levels and soil depth are presented in Table 2.

2.3. Prediction models

Following GlobalSoilMap specification (Arrouays et al., 2014) until 1 m depth, equal area splines were used to harmonize the SOC concentration and bulk density data for 5 depth intervals: 0–5, 5–15, 15–30, 30–60, and 60–100 cm. The smoothing parameter lambda chosen was 0.1 (Malone et al., 2009).

Table 1
Bulk density (t/m^3) for different land use and soil depths (cm), obtained from field measurements (10 soil pits) and pedotransfer functions.

Measured values	Depth 1	Depth 2	Depth 3	Depth 4	Depth 5
Vineyard	1.17 (11 cm)	1.20 (20 cm)	1.22 (35 cm)	–	–
Vineyard	1.14 (7 cm)	1.17 (16 cm)	–	–	–
Vineyard	1.13 (9 cm)	1.21 (34 cm)	1.22 (60 cm)	1.25 (81 cm)	–
Vineyard	1.16 (13 cm)	1.35 (35 cm)	1.17 (60 cm)	–	–
Forest	0.97 (25 cm)	1.07 (44 cm)	1.13 (63 cm)	1.23 (85 cm)	–
Forest	1.02 (20 cm)	1.08 (45 cm)	1.28 (75 cm)	–	–
Planted Forest	1.09 (15 cm)	1.27 (50 cm)	1.40 (82 cm)	1.33 (124 cm)	–
Pasture	1.15 (10 cm)	1.16 (33 cm)	1.25 (51 cm)	–	–
Arable Crops	1.10 (7 cm)	1.55 (30 cm)	1.44 (45 cm)	1.28 (73 cm)	–
Fallow	1.29 (40 cm)	1.33 (59 cm)	1.21 (94 cm)	1.16 (118 cm)	–

Pedotransfer functions[a]	Reference	RMSE
(1) $p_m = 1.35 + 0.0045 * sand + 6 * 10^{-5} * (44.7 - sand)^2 + 0.060 * \log depth$ $p_b = \frac{100}{(\frac{OM(\%)}{p_{OM}}) + (\frac{100 - OM(\%)}{p_m})}$	Tranter et al. (2007)	0.16
(2) $p_b = 1.5688 - 0.0005 * clay - 0.009 * OC$	Benites et al. (2007)	0.11
(3) 30–30 cm : $p_b = 1.5544 - 0.0004 * clay - 0.01 * OC + 0.0067 * SB$ 30–100 cm : $p_b = 1.5674 - 0.0005 * clay - 0.006 * OC + 0.0076 * SB$	Benites et al. (2007)	0.13

OC (g/kg): organic carbon; *SB* (cmolc/kg) — sum of basic cations (Ca^{2+}, Mg^{2+} and K^+); *clay* (g/kg).
[a] p_b = bulk density (g/cm^3); p_m: mineral bulk density (g/cm^3); p_{OM} = organic matter bulk density = 0.224 g/cm^3; *sand* (dag/kg); *depth* (cm).

Table 2
Variables used in the prediction of SOC content (g/kg) and soil depth of the study area in Vale dos Vinhedos in Rio Grande do Sul, Brazil.

Variables	Data descriptions	Type	Mean (min–max)	Soil carbon	Soil depth
Digital elevation model — 15 m	Elevation above mean sea level	Numeric	541.49 (206.15–723.05)	X	
Coordinate *X*	UTM latitude	Numeric	445052 (438242–451863)	X	
Coordinate *Y*	UTM longitude	Numeric	6770978 (6765083–6776873)	X	
Slope	Local hill slope gradient	Numeric	13.85 (0–81.01)	X	X
Aspect	Slope aspect	Numeric	180 (0–360)	X	X
Analytical hillshading	Angle between the surface and the incoming light beams	Numeric	0.93 (0–2.74)	X	X
TWI	Topographic wetness index	Numeric	3.12 (0.27–8.76)	X	X
LS factor	Slope length factor	Numeric	3.71 (0–95.9)	X	X
Vertical distance to channel network	Altitude above channel network	Numeric	26.86 (0–259.84)	X	X
Valley depth	Relative position of the valley	Numeric	24.48 (0.36–275.18)	X	X
Slope height	Vertical distance from the base of the slope to the crest	Numeric	24.91 (0.03–309.36)	X	X
Normalized height	Height position within a reference area	Numeric	0.49 (0–1)	X	X
Mid slope position	Cover the warmer zones of slopes	Numeric	0.52 (0–1)	X	
Flow direction	Direction of the flow	Numeric	35.06 (1–255)	X	X
MRVBF	Identifies the depositional areas	Numeric	0.21 (0–4.92)	X	X
Overland flow distance to channel network	Distance from non-channel cells to channel cells	Numeric	204.24 (0–1385)	X	X
Direct insolation	Potential incoming solar radiation	Numeric	3.29 (0–5.71)	X	
Soil order	Soil order map	Categorical	6 classes	X	X
Land use	Land use map	Categorical	6 classes	X	
Convexity	Terrain surface convexity	Numeric	0.51 (0.26–0.78)		X
Topographic position index (TPI)	Compare elevation of each cell to the neighborhood	Numeric	−0.05 (−11.14 to 21.97)		X
Mass balance index (MBI)	Balance between soil mass deposited and eroded	Numeric	0.16 (−0.81 to 1.61)		X
Plan curvature	Curvature in a horizontal plane	Numeric	0 (−0.16 to 0.31)		X
Vector ruggedness measure (VRM)	Measures terrain ruggedness	Numeric	0.01 (0–0.12)		X
LandMapR	Landform classification	Categorical	12 classes		X

The splined data were randomly split into 75% (122 pedons) for training the model, and 25% (41 pedons) for validation. The training data were used to predict SOC concentrations and all the pedons were used to predict soil depth. Four different regression models were tested: Multiple Linear Regression (MLR), Stepwise Multiple Linear Regression (SMLR), Cubist, and Random Forest.

In MLR, each independent variable is weighted by the regression to ensure maximal prediction from the set of independent variables (Hair et al., 2009). The weights denote relative contribution of the independent variables and facilitate to know the influence of each variable. However, correlation among independent variables needs to be considered. In SMLR, each variable is considered to be included prior to developing the equation. The independent variable with the greatest contribution is added first, followed by the variables selected based on their incremental contribution over the variables already in the equation (Hair et al., 2009). The Cubist model is based on the M5 algorithm of Quinlan (1992). The M5 algorithm builds tree-based models, which may have multivariate linear models at their leaves (Quinlan, 1992). It first partitions the data into subsets within which their characteristics are similar with respect to the target variable and the covariates. There are several rules arranged in hierarchy. The Random Forest is an ensemble learning method for classification (and regression) that operate by constructing a multitude of decision trees at training time which are later aggregated to give one single prediction for each observation in a dataset. For regression, the prediction is the average of the individual tree outputs (Breiman, 2001; Malone, 2013).

Based on similarity of results with the original values (Fig. 3), MLR proved to be the most robust model to predict SOC concentration and it was chosen to model SOC concentration and soil depth. Then, two sets of MLR models were implemented, one set for the SOC concentration (5 models, one for each depth) and one for the soil depth. Residual values (the difference between predicted and observed) were calculated for each model, and spatial relation was modeled with variograms. Kriging of the residuals was performed for the entire area, and the results were added to MLR estimation. The relative importance of the variables for each model was estimated based on absolute value of *t*-statistics. The final results for SOC concentration maps were refined replacing negative values by zero.

The soil depth map had values ranges between 0 and 250 cm. The map was sliced into 5 layers: 0–5 cm, 5–15 cm, 15–30 cm, 30–60 cm, 60–100 cm, creating 5 sets of thickness data. The thickness data were used to calculate SOC stocks, by each depth intervals.

The gravel and stone contents were obtained from the 163 pedons (Flores et al., 2012) and the distribution by depth was estimated by equal area splines. The values were extrapolated to the entire area through reference profiles of soil map units (Flores et al., 2012).

To calculate SOC stocks in t/ha, SOC concentrations in mass fraction were multiplied by bulk density previously calculated and mapped (Section 2.2) and thickness for each depth, and corrected for gravel and stone contents, according to the following equation:

$$\mathrm{SOC}\left[\frac{\mathrm{ton}}{\mathrm{ha}}\right] = \left[\left(\mathrm{SOC}\left[\frac{\mathrm{g}}{\mathrm{kg}}\right] \times \mathrm{BD}\left[\frac{\mathrm{g}}{\mathrm{cm^3}}\right] \times \mathrm{thickness}\,[\mathrm{cm}]\right)/10\right] \times \left(1 - \frac{\mathrm{gravels}\ [\%]}{100}\right). \quad (1)$$

To compare SOC stocks in soils under different land use and soil types, the results needed to be corrected by mass, avoiding carbon stock variation due to bulk density changes. The cumulative mass approach should be preferred as the basis for carbon stock accounting on a fixed mass per unit area (Minasny et al., 2013). The approach from Gifford and Roderick (2003) was used to calculate the cumulative mass and SOC stocks down to 1 m profile. This approach corrects SOC stocks using a reference cumulative mass. Soil mass of the forest areas were chosen as reference, as represent mass of soils under natural vegetation, and were calculated by the measured bulk density splined and the respective thickness. The reference mass by interval depth were 4.95 g/cm^2 for 0–5 cm, 9.9 g/cm^2 for 5–15 cm, 15.15 g/cm^2 for 15–30 cm, 33.6 g/cm^2 for 30–60 cm and 47.6 g/cm^2 for 60–100 cm. For the whole area, the soil mass for each depth was calculated by the bulk density maps and the thickness layers derived from the soil depth map. Then, the reference soil mass, the soil mass for each depth of the entire study area, and the previously calculated SOC stocks were each one cumulatively summed.

The cumulative corrected SOC stocks to the entire area, for each depth, were calculated through the equation applied to each pixel as follows:

$$c_s(t) = c_s(z_a) + \frac{c_s(z_b) - c_s(z_a)}{m_s(z_b) - m_s(z_a)}\left(m_s(t) - m_s(z_a)\right) \quad (2)$$

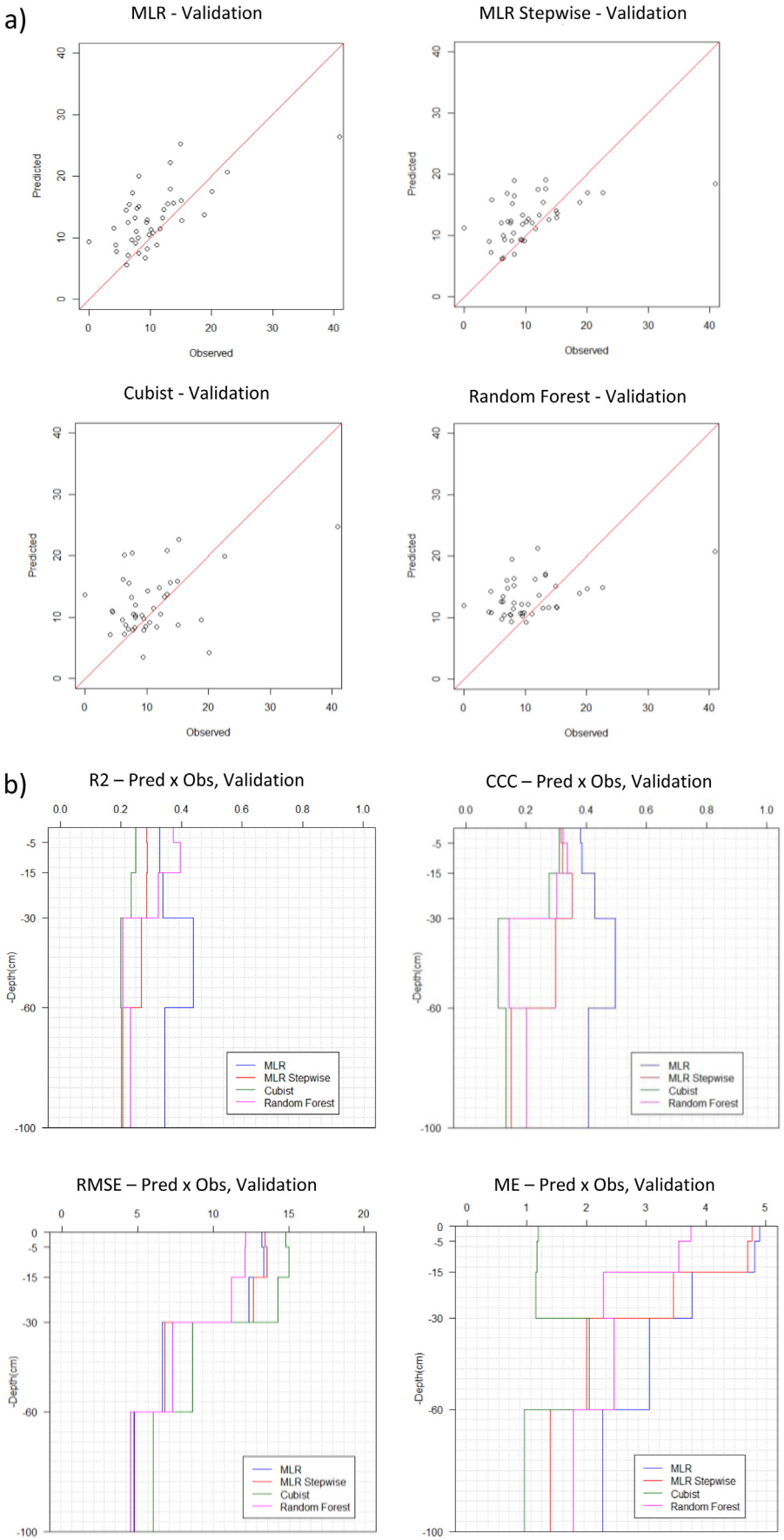

Fig. 3. a) Example of distribution of predicted × observed values, depth 30 to 60 cm, and b) validation of SOC concentration prediction for all depth intervals, by 4 different methods.

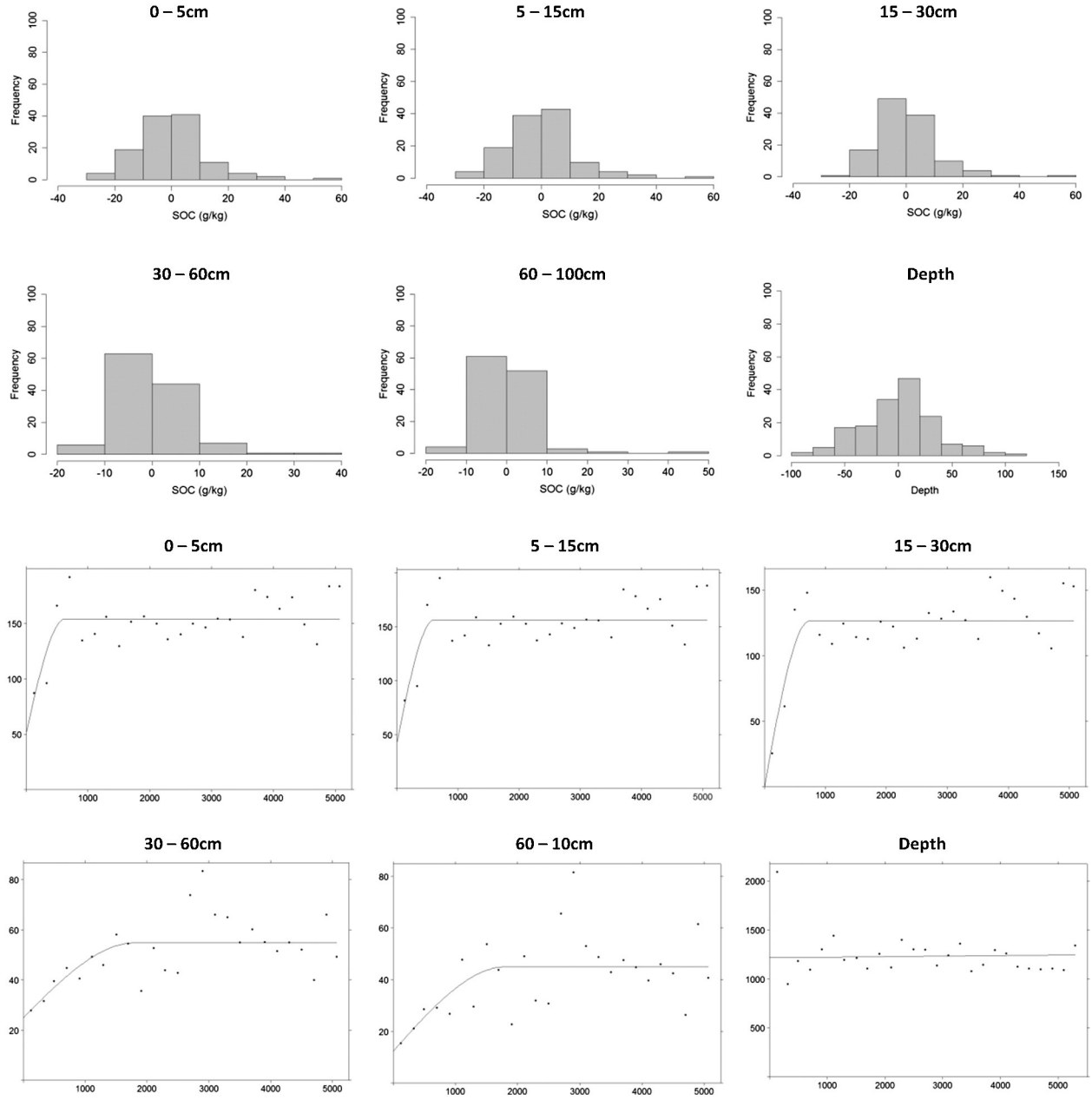

Fig. 4. Histograms and variograms of residuals (observed–predicted), from SOC concentration and depth predictions.

where $c_s(t)$ is the value of cumulative SOC stocks corrected by mass; $c_s(z_a)$ and $m_s(z_a)$ are the value of cumulative SOC stocks and mass, respectively, from the lower boundary of the layer above it; $c_s(z_b)$ and $m_s(z_b)$ are the cumulative SOC stocks and mass of the lower boundary of the current layer; $m_s(t)$ is the cumulative soil mass from the lower depth of the reference layer.

The SOC stocks for each interval depth was calculated by subtracting the cumulative SOC stocks of the lower and upper limit from respective layer.

2.4. Prediction evaluation

The SOC concentration models were validated with 25% of the data, and the soil depth model with the whole dataset, using 4 statistical parameters: RMSE, ME, R^2 and CCC. The R^2 is the coefficient of determination of linear regression, between the observed values and predicted values. RMSE correspond to root mean square error, ME to the mean error, and CCC to the Lin's Concordance Correlation Coefficient. The R^2 was obtained directly from the model in R, whereas other parameters were calculated as follows:

$$\mathrm{ME} = \frac{1}{n}\sum_{1=1}^{n} \hat{z}(x_i) - z(x_i) \tag{3}$$

$$\mathrm{RMSE} = \sqrt{\frac{1}{n}\sum_{i=1}^{n} [z(x_i) - \hat{z}(x_i)]^2} \tag{4}$$

$$\mathrm{CCC} = \frac{2 * \rho * \sigma_{\hat{z}(x_i)} * \sigma_{z(x_i)}}{\sigma^2_{\hat{z}(x_i)} + \sigma^2_{z(x_i)} + (\hat{z}(x_i) - z(x_i))^2} \tag{5}$$

where n is the number of the validation sample points, $z(x_i)$ is the observed value, $\hat{z}(x_i)$ is the predicted value, $\sigma^2_{z(x_i)}$ and $\sigma^2_{\hat{z}(x_i)}$ are the

Table 3
Descriptive statistics of training, validation, and estimated SOC content and soil depth.

SOC content		Training data $n = 122$ points	Validation data $n = 44$ points	Estimates $n = 312{,}790$ pixels
0–5 cm	Mean	27.5	24.7	31.5
	Median	23.8	22.7	31.1
	Min	4.6	7.0	0
	Max	93.5	61.0	103.8
5–15 cm	Mean	27.5	24.8	31.6
	Median	23.5	23.0	31.2
	Min	4.7	7.0	0
	Max	95.3	61.6	108.6
15–30 cm	Mean	23.3	21.9	26.5
	Median	19.9	20.7	25.9
	Min	4.6	7.0	0
	Max	90.3	59.6	176
30–60 cm	Mean	12.2	10.7	13.1
	Median	10.1	9.4	12.5
	Min	0	0	0
	Max	59.5	40.9	60.1
60–100 cm	Mean	7.7	6.4	9.1
	Median	6.1	5.9	8.6
	Min	0	0	0
	Max	59.5	26.2	59.5
Soil depth		$n = 163$ points	$n = 163$ points	$n = 312{,}790$ pixels
	Mean	149.4	149.4	148.7
	Median	150	150	150
	Min	25	25	0
	Max	250	250	250

variances, and ρ is the correlation coefficient between the predictions and observations. The impact of each variable was measured by the absolute value of t-statistics for each model parameter obtained through MLR.

2.5. Uncertainty and probability maps

Estimating uncertainty is complex considering all the sources of uncertainty. There are a number of approaches to estimate the uncertainty and Malone et al. (2011) and Shrestha and Solomatine (2006) suggest the empirical approach. In this approach, the residuals between modeled outputs and corresponding observed data are used to formulate prediction intervals (PIs). The uncertainty is expressed in the form of two quantiles of the underlying distribution of model error (residuals). The PI takes into account all sources of uncertainty and circumvents attempts to separate out the contribution of each source of uncertainty (Malone et al., 2011; Shrestha and Solomatine, 2006; Solomatine and Shrestha, 2009). The methodology is independent of the prediction model structure, as it requires only the model outputs.

Table 4
Validation of the Multiple Linear Regression and regression kriging for predicting SOC content (g/kg) and soil depth (cm).

Soil depth	Multiple Linear Regression				Regression kriging			
	R^2[a]	RMSE[a]	ME[a]	CCC[a]	R^2[a]	RMSE[a]	ME[a]	CCC[a]
0–5	0.33	13.23	4.89	0.38	0.34	12.82	4.09	0.39
5–15	0.33	13.36	4.80	0.38	0.33	13.00	3.97	0.39
15–30	0.34	12.37	3.76	0.43	0.35	12.00	3.10	0.45
30–60	0.44	6.62	3.04	0.49	0.48	5.80	2.44	0.58
60–100	0.34	4.77	2.26	0.41	0.41	4.44	1.87	0.52
Depth[b]	0.43	34.78	0	0.59	–	–	–	–

[a] R^2 = coefficient of determination, RMSE = root mean square error, ME = mean error, CCC = Lin's Concordance Correlation Coefficient.
[b] Depth model used the whole data samples, and the validation was made based on training data.

We used the empirical approach estimating PIs through the residuals of SOC predictions. Between several methods for modeling the distribution of residuals, we chose sequential Gaussian geostatistical simulations because it is more related to the spatial method used for SOC prediction.

Firstly, the residuals from MLR prediction of SOC, at each 5 standard depth, were simulated with 100 iterations and then the outputs were added back to the predicted SOC concentration. For each predicting pixel, we considered the two percentiles, lower 5% and upper 95%, covering the 90% PI, as suggested in GlobalSoilMap specifications (Arrouays et al., 2014). Lower and upper limits were mapped (Fig. 5) and the uncertainty models were evaluated on the 25% validation dataset (Fig. 9).

With the 100 values of SOC concentration, we applied Eq. (1) for produced SOC stocks and Eq. (2) to correct by cumulative mass. The results were used to produce maps of probability of total SOC stock (0–100 cm) that exceed a threshold of 184 t C/ha. The value of 184 t C/ha is based on the averaged SOC stocks under forest for the entire study area. Areas with high probability of exceeding this limit are likely to have the same SOC stocks as under forest. The number of times that pixels values exceeded the threshold, between 100, was counting and recording for producing the maps. The following probabilities were considered for mapping: 20%, 40%, 60% and 80%.

2.6. SOC changes

SOC changes due to land use changes were estimated using Projected Natural Vegetation Soil Carbon (PNVSC) approach (Waring et al., 2014). PNVSC is considered a projected SOC that could be present today if the area was under natural vegetation.

The PNVSC maps were elaborated re-applying the equations produced by MLR models for SOC concentration (Section 2.3), nevertheless with the coefficients for land use types other than forest set to zero. The produced maps are hypothetically representing soil carbon which could be observed today if the whole study area remained under natural vegetation. The predicted SOC concentration can now to be compared with PNVSC by Eq. (6) to estimate SOC changes due to land use change (e.g. Adhikari and Hartemink, 2015):

$$SOC_{changes} = SOC_{predicted} - PNVSC. \quad (6)$$

Negative SOC change indicates that the soil has less SOC compared to the projected natural vegetation (forest) whereas positive SOC change indicate that the soils have accumulated SOC.

3. Results

3.1. SOC prediction and model comparison

While comparing four prediction methods using the training data, Cubist and Random Forest showed a high R^2 (>0.92) and CCC (>0.8) for SOC prediction at all depths, compared to MLR and SMLR with lower values (R^2 < 0.51 and CCC < 0.64). Similarly, both Cubist and Random Forest had lower RMSE (<6.4 g/kg) than MLR and SMLR (RMSE > 6.7), when comparing all the soil depths.

However, when using the validation samples (25% of pedons), MLR had a higher R^2 and CCC and a lower RMSE than the other models (Fig. 3b). Comparing the distribution of observed and predicted values (Fig. 3a), MLR had less spread of points. The MLR model suffered from the higher bias (ME) compared to all other methods. RMSE did not differ much between methods with Cubist showing the highest RMSE at all depths.

Based on R^2 and CCC values, and considering the RMSE not so different between methods, MLR was the best model to estimate the SOC concentration. The high bias indicates that MLR might overestimate the predicted values and, therefore, it should be considered when interpreting the results. Based on these findings, we assumed that

MLR could be the appropriate method for SOC concentration and soil depth prediction.

After the predictions were made by the MLR models, the distribution of prediction residuals and their spatial dependence was analyzed and plotted (Fig. 4). Spatially, the residuals were poorly auto-correlated for the top three depths (0–5, 5–15, and 15–30 cm), whereas a better spatial structure was observed below 30 cm soil depth. Residuals of soil depth prediction were normally distributed with no spatial auto-correlation as suggested by the pure nugget effect of the variogram.

3.2. Evaluation of MLR model for SOC and soil depth prediction

Descriptive statistics of training data, validation data, and the estimates are shown in Table 3. The mean SOC concentration for the validation are slightly lower than for training data. The estimated data have higher mean, median and maximum values than the training data which suggests that the MLR model can overestimate SOC concentration. The bias of MLR is depicted in Fig. 3b and in Table 4, showing higher values at 0–5 cm soil depth and decreasing until depth 60–100 cm. For the soil depth, the mean of estimated data were similar to training data.

Validation results of the MLR model is shown in Table 4. The R^2 between predicted and measured values differed by depth and was highest at 30–60 cm, with value of 0.44, and CCC of 0.49. For all other depths, R^2 was between 0.33 and 0.34, and values of CCC were between 0.38 and 0.43. The RMSE and ME decreased with increasing soil depth. When the residuals were added to the MLR predictions, the R^2 and CCC increased and RMSE and ME decreased (Table 4).

For the soil depth prediction model, CCC of 0.59, R^2 of 0.43, and RMSE of about 34.8 cm were observed. The high values of R^2 and CCC were probably due to the use of same samples for model training and validation.

3.3. Spatial predictions and variable importance

In general, SOC levels differed by depth, soil order and by land use type. SOC concentration decreased below 15 cm depth (Table 5 and Fig. 5). The mean values (Table 5) vary between 5.8 g C/kg, from vineyard areas in Alfisols at 60–100 cm depth, and 43.9 g C/kg, from pasture areas in Entisols at 15–30 cm depth. Entisols have the highest mean SOC concentration, 39.1 g C/kg at 5–15 cm depth and Alfisols the lowest, 7.1 g C/kg at depth 60–100 cm (Table 7). Similarly, forest has the highest mean SOC concentration, 36.1 g C/kg at 5–15 cm depth, and arable crops the lowest, 6.7 g C/kg, at depth 60–100 cm.

The importance of the variables for SOC concentration prediction differed by depth. The relative importance of the 15 main variables in SOC concentration and the soil depth model is presented in Fig. 6. Up to 30 cm soil depth, the most important variable was Soil Order (Entisols), coordinate *X*, Aspect and DEM. Below that soil depth the important variables were as follows: Overland Flow Distance to Channel Network, Aspect, Soil Order (Entisols and Oxisols), coordinate *Y*, and Normalized Height. Overall, the Entisols soil order was a good predictor.

Descriptive statistics of soil depth data and its prediction are shown in Table 3, and the predicted map in Fig. 7. Soils shallower than 70 cm occupied 1% of area (81 ha) and most of them were Entisols (65%) and Mollisols (33%). Soils deeper than 200 cm occupied 5% of area (439 ha) and most of them were Ultisols (54%) and Mollisols (20%). Soils between 70 and 200 cm occupied the largest area (94%) and most of them were Inceptisols (43%), Ultisols (28%), and Mollisols (16%). The deepest soils were Ultisols (169 cm), followed by Oxisols (158 cm), Inceptisols (150 cm), Alfisols (142 cm), Mollisols (134 cm) and Entisols (110 cm). Soil depth increased in the northern part of the study area and it varied mainly with slope as shallower soils were found on steeper slopes.

Table 5
Predicted SOC content (g/kg) by soil order and land use types, from the study area in Vale dos Vinhedos in Rio Grande do Sul, Brazil.

Soil order	Land use	0–5 cm	5–15 cm	15–30 cm	30–60 cm	60–100 cm
Alfisol	Arable crops	26.1 (±1.4)	26.0 (±1.4)	19.3 (±2.2)	10.2 (±2.4)	7.8 (±1.6)
	Fallow	27.2 (±5.1)	26.7 (±5.2)	17.5 (±5.8)	10.5 (±5.2)	7.9 (±4.2)
	Forest	28.1 (±5.4)	27.9 (±5.5)	18.8 (±5.7)	8.7 (±4.8)	8.5 (±4.2)
	Pasture	18.8 (±6.2)	19.0 (±6.1)	18.3 (±5.7)	12.0 (±5.0)	9.2 (±4.6)
	Planted forest	–	–	–	–	–
	Vineyard	20.5 (±5.3)	20.2 (±5.4)	13.7 (±5.5)	7.9 (±4.5)	5.8 (±3.8)
Entisol	Arable crops	41.3 (±0.7)	41.7 (±0.7)	36.1 (±0.7)	16.2 (±1.2)	13.0 (±1.0)
	Fallow	37.9 (±8.7)	38.0 (±8.9)	33.1 (±9.1)	17.3 (±5.0)	11.0 (±4.3)
	Forest	43.1 (±8.7)	43.7 (±8.9)	40.9 (±10.4)	16.9 (±6.4)	11.9 (±5.4)
	Pasture	39.5 (±8.2)	40.4 (±8.3)	43.9 (±8.2)	24.7 (±4.5)	15.4 (±3.7)
	Planted forest	30.8 (±5.3)	31.2 (±5.4)	31.1 (±5.6)	16.8 (±6.9)	9.2 (±5.5)
	Vineyard	31.5 (±6.9)	31.7 (±7.1)	29.1 (±7.8)	13.8 (±5.3)	7.9 (±4.2)
Inceptisol	Arable crops	29.2 (±4.9)	29.3 (±5.0)	24.8 (±5.5)	13.4 (±4.9)	7.8 (±3.8)
	Fallow	33.6 (±6.3)	33.2 (±6.3)	25.1 (±6.4)	13.8 (±5.7)	8.9 (±5.8)
	Forest	37.0 (±7.0)	37.0 (±7.1)	29.7 (±7.0)	14.2 (±6.1)	11.8 (±6.0)
	Pasture	33.2 (±6.4)	33.7 (±6.4)	34.2 (±6.3)	21.8 (±5.3)	15.3 (±4.6)
	Planted forest	24.9 (±4.1)	25.0 (±4.2)	23.4 (±4.2)	17.6 (±4.2)	12.0 (±4.3)
	Vineyard	27.4 (±7.0)	27.3 (±7.1)	21.9 (±6.9)	12.2 (±5.6)	7.8 (±4.9)
Mollisol	Arable crops	27.5 (±9.3)	27.5 (±9.4)	22.0 (±8.4)	10.6 (±4.5)	5.7 (±3.5)
	Fallow	33.7 (±7.4)	33.4 (±7.7)	25.2 (±8.8)	12.9 (±5.0)	6.8 (±4.0)
	Forest	37.0 (±8.5)	37.3 (±8.7)	31.4 (±9.0)	11.1 (±5.3)	7.5 (±3.7)
	Pasture	32.4 (±11.3)	32.6 (±11.5)	31.4 (±10)	17.3 (±3.0)	9.8 (±2.4)
	Planted forest	19.7 (±3.2)	19.9 (±3.2)	19.8 (±4.1)	12.6 (±3.3)	7.3 (±2.5)
	Vineyard	29.4 (±8.9)	29.3 (±9.1)	23.5 (±9.3)	11.7 (±5.4)	6.4 (±3.8)
Oxisol	Arable crops	32.1 (±4.8)	32.2 (±5.0)	33.4 (±5.5)	28.8 (±3.6)	9.1 (±2.8)
	Fallow	38.6 (±3.3)	38.3 (±3.5)	34.9 (±4.7)	29.8 (±3.0)	13.5 (±2.2)
	Forest	40.2 (±6.9)	40.1 (±6.9)	37.1 (±6.1)	28.5 (±4.7)	12.2 (±3.6)
	Pasture	34.2 (±4.6)	34.4 (±4.7)	39.9 (±4.9)	34.6 (±3.7)	13.4 (±3.3)
	Planted forest	–	–	–	–	–
	Vineyard	33.5 (±4.7)	33.5 (±4.7)	33.7 (±4.4)	29.9 (±3.3)	11.8 (±2.7)
Ultisol	Arable crops	21.6 (±6.7)	21.8 (±6.7)	19.6 (±6.1)	11.9 (±5.1)	5.6 (±3.4)
	Fallow	27.7 (±5.8)	27.5 (±5.9)	22.4 (±6.4)	13.5 (±4.4)	8.6 (±3.8)
	Forest	30.8 (±7.1)	31.0 (±7.3)	26.3 (±7.8)	12.5 (±5.2)	9.8 (±4.6)
	Pasture	25.5 (±6.9)	26.1 (±7.0)	29.0 (±6.6)	19.5 (±3.7)	12.5 (±3.0)
	Planted forest	17.5 (±3.7)	17.7 (±3.7)	19.5 (±3.6)	16.1 (±3.2)	9.9 (±2.6)
	Vineyard	21.6 (±6.9)	21.7 (±7.1)	19.3 (±7.4)	11.3 (±4.7)	6.8 (±3.9)

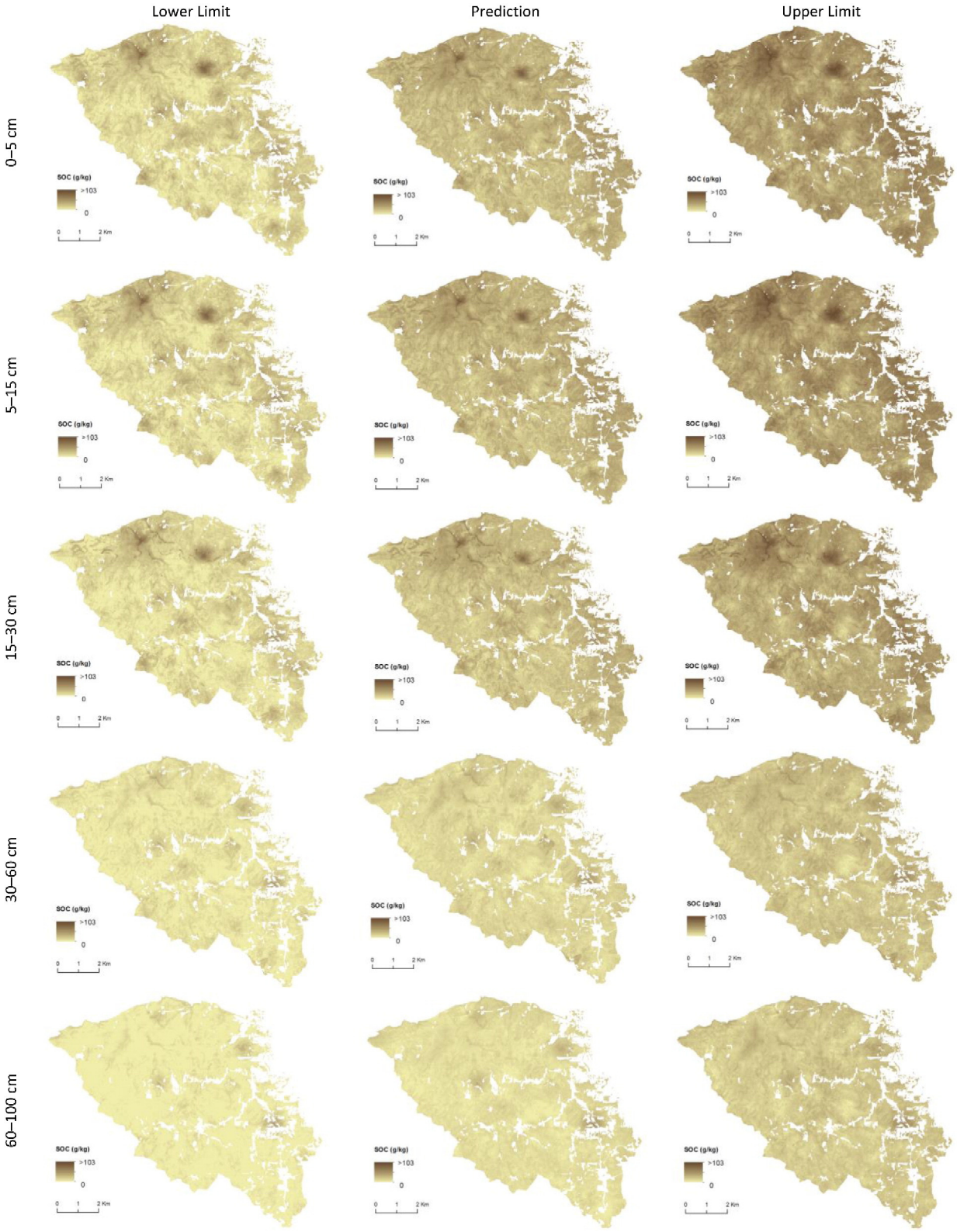

Fig. 5. Prediction of SOC content (g/kg) and lower (5%) and upper limit (95%) for five soil depths of Vale dos Vinhedos in Rio Grande do Sul, Brazil.

Pedotransfer function estimated bulk density for all the pedons, with average of 1.17 g/cm^3 (0–5 cm), 1.18 g/cm^3 (5–15 cm), 1.19 g/cm^3 (15–30 cm), 1.26 g/cm^3 (30–60 cm) and 1.27 g/cm^3 (60–100 cm). The values ranged between 0.54–1.4 g/cm^3 (0–5 cm), 0.56–1.4 g/cm^3 (5–15 cm), 1.19–1.4 g/cm^3 (15–30 cm), 1.26–1.47 g/cm^3 (30–60 cm) and 1.27–1.47 g/cm^3 (60–100 cm).

Fig. 8 shows SOC stock maps for each 5 depth, and the total stock for 0–100 cm. Overall, it appeared that the spatial distribution of SOC stocks was similar to SOC concentration. Values were higher on the valley banks and bottom valley, which were under forest and with reduced agricultural use. Total SOC stocks were highest in Oxisols (230–280 t C/ha) and lower in Alfisols (104–143 t C/ha), as in Table 6. Soils under pasture

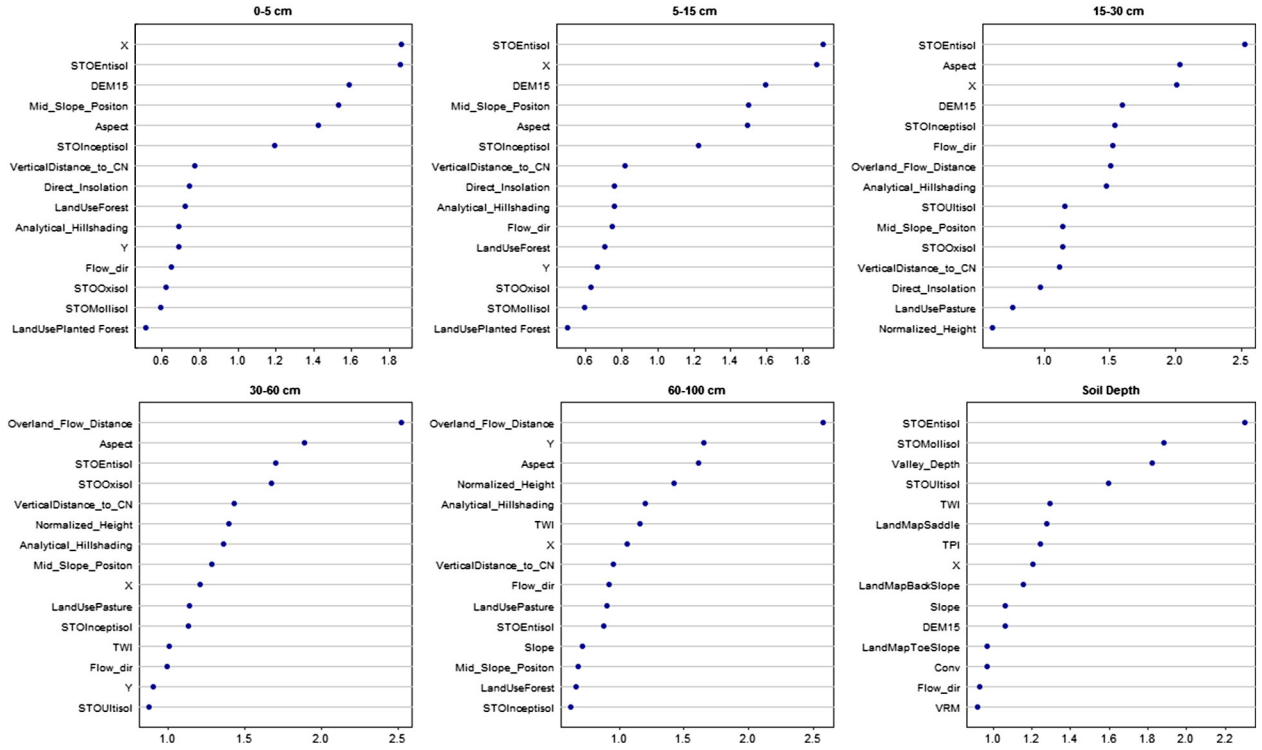

Fig. 6. Relative importance of the 15 variables used for predicting SOC content at each soil depth. The importance is calculated based on the absolute value of the *t*-statistics for each model parameter (see Table 1 for a description of the variables).

areas had the highest SOC stocks (139–280 t C/ha) and soils under planted forest areas the lowest SOC stocks (116–174 t C/ha). Oxisols under pasture areas had the highest SOC stocks (280 t C/ha) and Alfisols under vineyard the lowest (104 t C/ha).

3.4. Uncertainty and probability maps

For uncertainty of SOC concentrations prediction, calculated by empirical approach and mapped (Fig. 5), the averages for the lower limit of

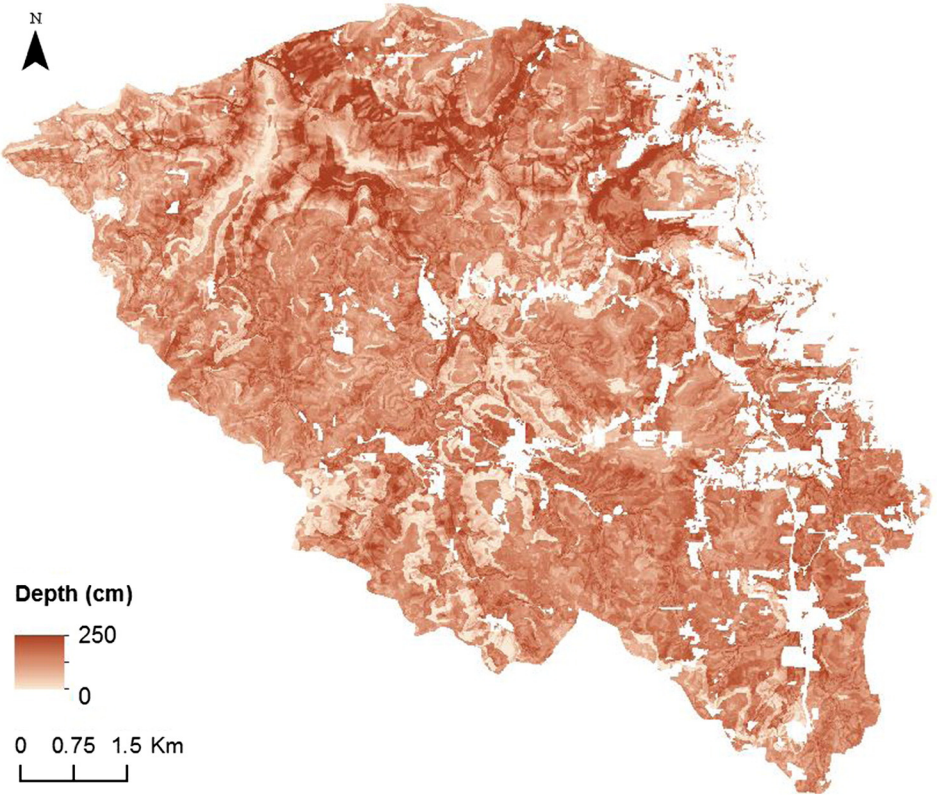

Fig. 7. Soil depth of the study area in Vale dos Vinhedos in Rio Grande do Sul, Brazil.

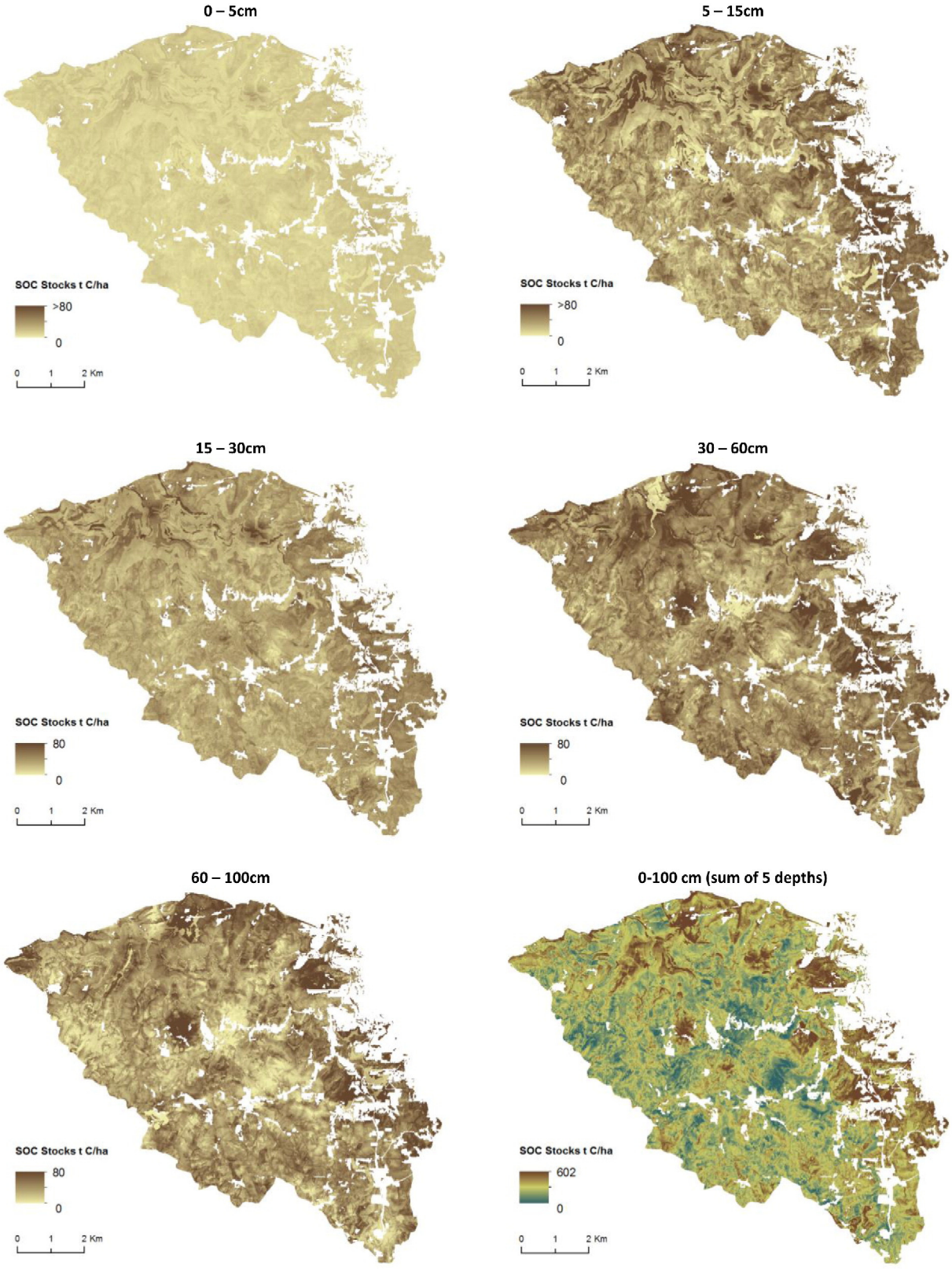

Fig. 8. Estimation of SOC stocks (t C/ha) of the study area in Vale dos Vinhedos in Rio Grande do Sul, Brazil.

prediction decreased from 10.5 g C/kg at 0–5 cm soil depth to 1.5 g C/kg at 60–100 cm depth. The means for upper prediction limit decreased from 53.8 g C/kg at 0–5 cm soil depth to 19.4 g C/kg at 60–100 cm soil depth. A similar trend was found for the difference in the lower and upper limits.

The uncertainty values of nine sample points, from the validation dataset (25% of pedons), are shown in Fig. 9. The blue line represents estimated value, and red lines represent the low (left) and the upper limit (right) for the 5 depths. Bars represent the splined SOC values, harmonized by depth of GlobalSoilMap. The prediction intervals are higher

Table 6
Calculated SOC stocks (t C/ha) by soil order and land use types for the study area in Vale dos Vinhedos in Rio Grande do Sul, Brazil.

Soil order	Land use	0–5 cm	5–15 cm	15–30 cm	30–60 cm	60–100 cm	Total 0–100 cm
Alfisol	Arable crops	13 (±1)	25 (±2)	30 (±3)	40 (±7)	34 (±9)	143 (±18)
	Fallow	12 (±2)	23 (±4)	26 (±7)	39 (±17)	38 (±19)	137 (±46)
	Forest	11 (±3)	23 (±5)	27 (±7)	36 (±14)	39 (±19)	135 (±43)
	Pasture	8 (±3)	16 (±6)	25 (±9)	45 (±15)	45 (±19)	139 (±50)
	Planted forest	–	–	–	–	–	–
	Vineyard	9 (±2)	17 (±5)	20 (±7)	30 (±14)	29 (±18)	104 (±40)
Entisol	Arable crops	17 (±1)	34 (±3)	45 (±4)	46 (±10)	54 (±10)	197 (±15)
	Fallow	14 (±4)	28 (±8)	40 (±10)	51 (±16)	37 (±18)	170 (±39)
	Forest	16 (±4)	33 (±8)	51 (±15)	58 (±28)	36 (±20)	194 (±57)
	Pasture	14 (±4)	28 (±8)	49 (±12)	71 (±28)	50 (±23)	212 (±54)
	Planted forest	12 (±3)	24 (±6)	37 (±9)	47 (±30)	28 (±22)	147 (±60)
	Vineyard	12 (±3)	23 (±6)	35 (±9)	42 (±22)	28 (±18)	140 (±44)
Inceptisol	Arable crops	13 (±3)	26 (±6)	35 (±9)	47 (±15)	40 (±18)	160 (±44)
	Fallow	14 (±3)	29 (±7)	35 (±9)	48 (±18)	43 (±27)	170 (±55)
	Forest	15 (±4)	31 (±8)	40 (±10)	51 (±19)	52 (±26)	189 (±56)
	Pasture	14 (±4)	29 (±8)	46 (±10)	73 (±18)	72 (±22)	235 (±55)
	Planted forest	11 (±3)	22 (±5)	32 (±8)	55 (±16)	54 (±18)	174 (±43)
	Vineyard	11 (±3)	23 (±7)	30 (±9)	42 (±17)	38 (±21)	144 (±49)
Mollisol	Arable crops	11 (±3)	22 (±6)	27 (±9)	29 (±12)	22 (±13)	111 (±38)
	Fallow	12 (±3)	24 (±6)	29 (±9)	42 (±18)	30 (±19)	137 (±44)
	Forest	11 (±4)	22 (±9)	30 (±11)	45 (±17)	36 (±17)	144 (±43)
	Pasture	11 (±3)	23 (±6)	34 (±8)	51 (±12)	36 (±18)	155 (±36)
	Planted forest	7 (±2)	14 (±5)	21 (±7)	42 (±10)	33 (±11)	116 (±27)
	Vineyard	11 (±4)	21 (±8)	27 (±12)	38 (±18)	27 (±16)	124 (±49)
Oxisol	Arable crops	16 (±2)	32 (±5)	50 (±8)	95 (±12)	37 (±14)	230 (±38)
	Fallow	19 (±2)	38 (±3)	53 (±7)	100 (±10)	59 (±10)	268 (±30)
	Forest	20 (±3)	40 (±7)	56 (±9)	95 (±15)	53 (±18)	263 (±49)
	Pasture	17 (±3)	33 (±5)	59 (±9)	113 (±14)	58 (±15)	280 (±40)
	Planted forest	–	–	–	–	–	–
	Vineyard	17 (±2)	33 (±5)	51 (±7)	100 (±11)	51 (±13)	251 (±33)
Ultisol	Arable crops	10 (±3)	21 (±6)	29 (±8)	43 (±16)	31 (±16)	135 (±44)
	Fallow	13 (±3)	26 (±6)	34 (±9)	50 (±14)	44 (±18)	167 (±44)
	Forest	14 (±3)	28 (±7)	38 (±10)	49 (±16)	47 (±21)	176 (±50)
	Pasture	12 (±3)	24 (±6)	41 (±9)	70 (±13)	64 (±14)	212 (±39)
	Planted forest	8 (±2)	17 (±4)	28 (±6)	56 (±10)	53 (±13)	162 (±29)
	Vineyard	10 (±3)	20 (±6)	28 (±10)	42 (±16)	36 (±19)	136 (±47)

in upper layers than in lower layers. Of the 41 validation samples the following number were within prediction intervals: 36 for 0–5 cm depth, 34 for 5–15 cm depth, 34 for 15–30 cm depth, 38 for 30–60 cm depth, and 39 for 60–100 cm soil depth. More than 90% of the validation samples were within the prediction intervals derived from residuals with higher spatial covariance (30–60 cm and 60–100 cm).

For SOC stocks, the probability maps (Fig. 10) show areas where the SOC stock exceeds the threshold value at 20, 40, 60 and 80% probabilities. The probability for SOC stocks exceeding the limit is highest in the valley bottoms and in the eastern part of study area. There is an 80% probability of SOC stocks to exceed 184 t C/ha in about 13% (1029 ha) of the area.

3.5. SOC changes

The mean values of SOC predictions and PNVSC values are given in Table 7 where the data were aggregated by soil order and land use. Areas where SOC has been lost as compared to the same soils under forest are given in bold. SOC has been lost at 0–5 and 5–15 cm soil depth for all soil orders and land use types (except forest which was used as a reference). This loss is also observed at 15–30 cm and 60–100 cm depth, except for Oxisols and pasture. At 30–60 cm soil depth SOC levels has been increased in all soil orders and land use types. The maps of PNVSC and SOC changes are given in Fig. 11.

4. Discussion

This study predicted SOC concentration and SOC stocks in a subtropical area under different land use and a range of soil orders. The impact of land use on soil C was evaluated by comparing the SOC concentration under current use with a projected SOC that could be present today if the area was under natural vegetation. In this discussion, we shall focus on the methods of prediction, the effect of the variables used for prediction, and the distribution of SOC under different land uses and soil types.

4.1. Prediction model

The different methods tested for regression showed that model evaluation it's more reliable when using a separate validation dataset. Predicted values might be very similar to observed values, when considering the training model. This model may overfit the data and the performance can be poor using validation data. Minasny and McBratney (2013), observing the behavior of a random forest model, concluded that it can easily overfit the data. In our study, the Cubist and Random Forest models seem to overfit the data, whereas MLR produced estimation closer to validation data.

SOC concentrations were predicted based on regression kriging Model (MLR and kriging of residuals). The prediction showed the variation in SOC concentration spatially and by depth, land use and soil order. The model explained only part of the variation and when comparing the estimated mean, median and maximum values, our estimation from the model produced slightly higher SOC concentration than training data. This can be explained by the biased estimate when using a non-probability sample to calibrate the model or also some regions of the feature space to be over or under-represented in the training data.

The values of validation parameters such as R^2 and CCC were higher for 30–60 cm soil depth and were lower at other depth intervals. The

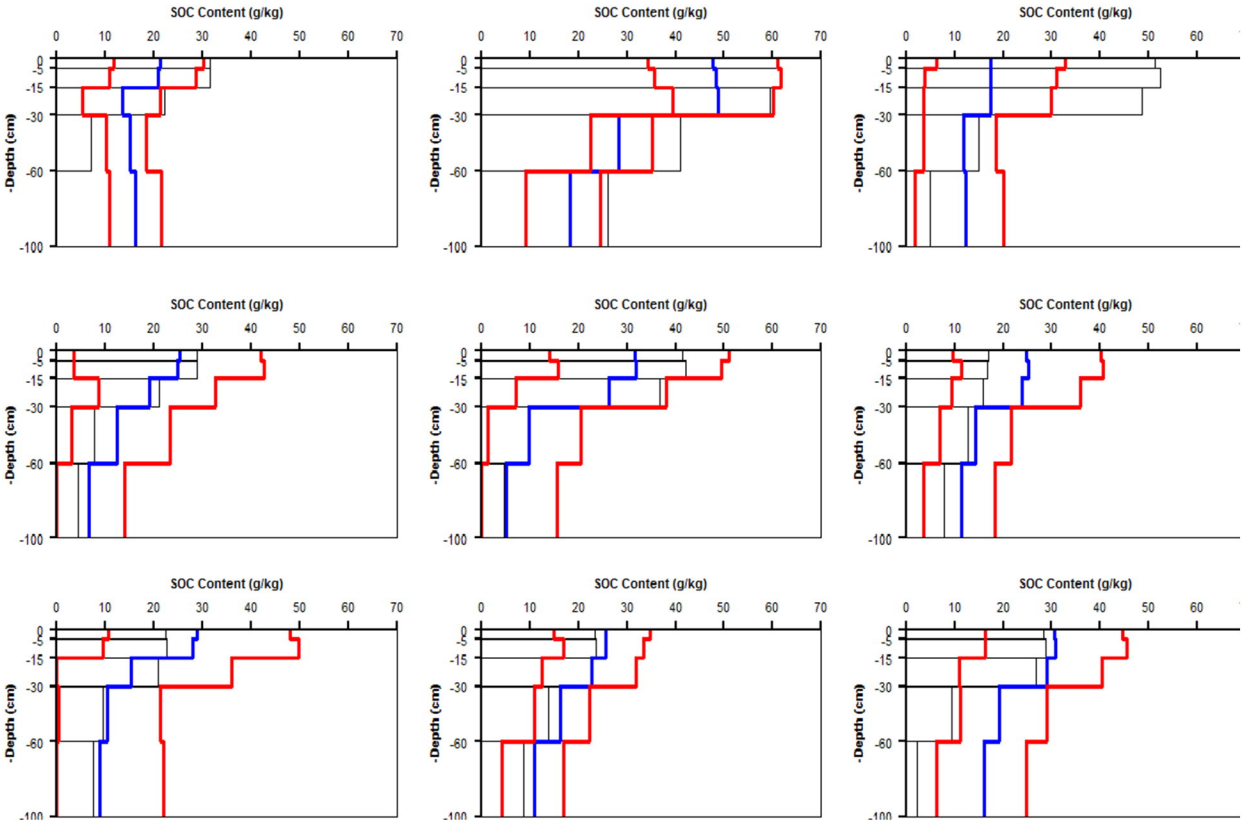

Fig. 9. Examples of uncertainty prediction intervals, for SOC levels, of 9 independent validation points. Predicted SOC values are shown in blue, and the lower (5%) and upper limit (95%) in red. Bars represent the SOC values of validation points obtained from spline functions, and harmonized by GlobalSoilMap depths. (For interpretation of the references to color in this figure legend, the reader is referred to the web version of this article.)

validation results, in Table 4, are comparable to most recent studies predicting SOC. For example, on temperate areas, Adhikari et al. (2014) found the model could explain 43% of variation in validation data, whereas Malone et al. (2009) found R^2 values of validation points ranging between 20% and 27%. Other studies present similar results (Brogniez et al., 2014; Collard et al., 2014; Forges et al., 2014; Wiesmeier et al., 2014).

The soil depth model could explain 43% of the variation, using all data for estimation and validation. The soil depth map followed the topographic variation, showing the deeper soils in valley bottom. The calculated bulk density varied between 0.54 and 1.47 g/cm^3 and were similar to the values found by Tornquist et al. (2009a), between 0.4 and 1.4 g/cm^3.

4.2. Importance of predictor variables

The relative importance of each variable was evaluated by absolute *t*-values. The *t*-value is model dependent, which means that if two or more variables are correlated with SOC concentration, and also correlated with each other, then only one variable may appear with the high *t*-value.

We noted that variable importance differed by soil depth. Up to 30 cm soil depth, the covariates Soil Order, coordinate *X*, Aspect and DEM were good predictors. Soil Order (Entisols) contributed mainly due its consistent higher SOC values (Table 5). There was a decrease in SOC concentration towards the west (Fig. 5) and hence coordinate *X* was important to identify this variation in east–west direction. There was a higher SOC concentration in the soils of the north in the valley bottom, and coordinate *Y* identifies this variation. In correlation analysis, it was noted that *Y* has a correlation of −0.47 with *X*, which is fairly high compared to other covariates. Both coordinates could explain the spatial variation of SOC concentration, although only *X* showed high *t*-value, and to separate individual effect in prediction is not straightforward (Hair et al., 2009). The north-facing slopes receive more solar radiation, and as a result possibly enhanced SOC decomposition and lower SOC levels. This effect can be seen at slightly higher SOC values in the northeast (slope south-facing) compared to the southwest (slope north-facing). This variation could be identified by the Aspect covariate.

At lower elevation, temperatures increases and likely the soils contain less carbon due to higher rates of decomposition. However, the elevation was a proxy for deposited material and areas at lower elevation had deeper soils with more SOC. There was a relatively high and negative correlation (−0.55) between DEM and Valley Depth. Only DEM is showed with high *t*-value, but both explain the SOC variation related with elevation.

For the layers below 30 cm soil depth the covariates Overland Flow Distance, Aspect, Soil Order, coordinate *Y*, and Normalized Height were important predictors for SOC concentration. Overland flow distance to channel network indicate that the SOC concentration is higher closer to channel network, possibly because of organic material deposits under dense vegetation. Libohova et al. (2014) found that areas with water accumulation for longer time periods stored 50–68% more total SOC compared to drier areas. Noticeable influence of soil orders covariates (Entisol, Oxisol or Inceptisol) in SOC prediction was found up to 60 cm depth but not below this depth. The coordinate *Y* is consistent with the valley bottom in north direction. The Normalized Height indicates the height relatively to the highest and lowest position within an area (Dietrich and Böhner, 2008) and this covariate correlates with Overland Flow Distance to Channel Network (0.63).

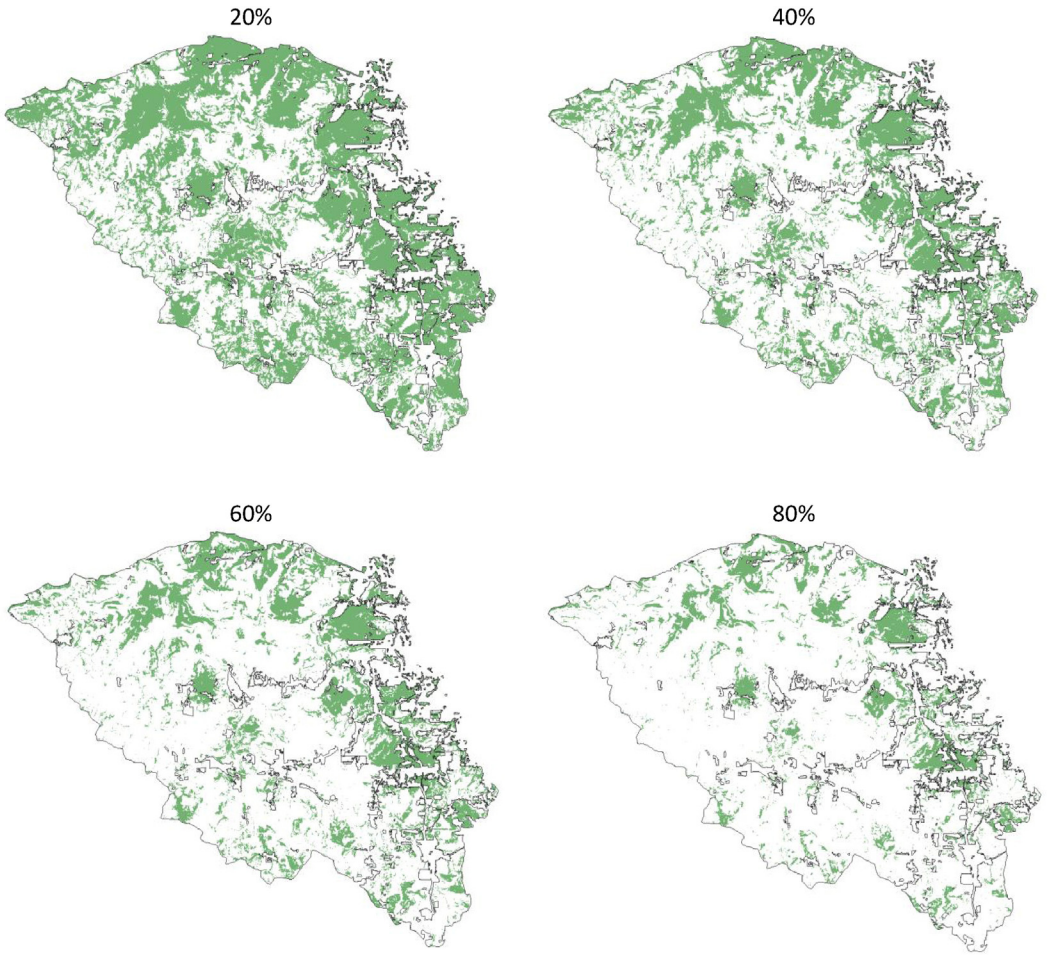

Fig. 10. Maps of different probabilities that the soil contain at least 184 ton SOC/ha in Vale dos Vinhedos in Rio Grande do Sul, Brazil.

For prediction of soil depth, Soil Order (Entisol, Mollisol and Ultisol) and Valley Depth proved good predictors. The Entisols are shallower soils (mean depth 110 cm) and Mollisols and Ultisols are the deeper soils. Although Oxisols are also deep soils, it had no significant impact on the soil depth model possibly because of the limited number of samples.

4.3. SOC concentration and stocks

The SOC concentration predicted for soils under forest and pasture differed by depth. In the upper layers, soils under forest had higher values whereas soils under pasture had more SOC with depth (Tables 5 and 7). Forest has larger amounts of litter and

Table 7
Predicted SOC content and Projected Natural Vegetation Soil Carbon (PNVSC), by soil order and land use. Figures in bold indicate that SOC was lost based on the PNVSC approach (SOC content predicted − PNVSC).

SOC and PNVSC (g/kg) — mean values (±standard deviation)										
Soil order	0–5 cm	PNVSC	5–15 cm	PNVSC	15–30 cm	PNVSC	30–60 cm	PNVSC	60–100 cm	PNVSC
Alfisol	**24.2 (±6.5)**	27.0 (±5.0)	**23.9 (±6.6)**	26.8 (±5.0)	**16.2 (±6.1)**	17.6 (±3.8)	8.4 (±4.7)	7.2 (±2.8)	**7.1 (±4.2)**	7.3 (±2.7)
Entisol	**38.7 (±9.7)**	42.1 (±6.6)	**39.1 (±10.0)**	42.6 (±6.7)	**36.4 (±11)**	38.5 (±5.9)	15.9 (±6.2)	15.5 (±4.8)	**10.5 (±5.3)**	10.8 (±4.0)
Inceptisol	**32.3 (±8.3)**	35.9 (±6.4)	**32.2 (±8.4)**	35.9 (±6.5)	**26.0 (±7.9)**	28.0 (±5.2)	13.5 (±6.0)	12.6 (±4.7)	**9.9 (±5.8)**	10.3 (±4.6)
Mollisol	**35.0 (±9.2)**	36.6 (±6.0)	**35.2 (±9.4)**	36.8 (±6.1)	**29.3 (±9.7)**	29.9 (±5.3)	11.4 (±5.3)	11.0 (±3.5)	**7.3 (±3.8)**	7.8 (±2.6)
Oxisol	**35.1 (±6.1)**	38.2 (±3.1)	**35.1 (±6.1)**	38.1 (±3.1)	35.7 (±5.7)	35.5 (±4.0)	30.3 (±4.4)	26.9 (±3.0)	11.8 (±3.3)	11.7 (±1.8)
Ultisol	**26.4 (±8.1)**	29.7 (±5.8)	**26.5 (±8.2)**	29.9 (±5.8)	**23.0 (±8.1)**	24.8 (±4.9)	12.4 (±5.1)	11.3 (±3.5)	**8.5 (±4.4)**	8.9 (±3.0)
Land use										
Arable Crops	**25.4 (±7.8)**	29.5 (±4.3)	**25.5 (±7.9)**	29.5 (±4.3)	**23.3 (±8.1)**	24.4 (±3.7)	15.2 (±8.1)	13.9 (±3.1)	**6.7 (±3.7)**	9.1 (±2.0)
Fallow	**30.9 (±7.2)**	32.2 (±3.9)	**30.7 (±7.3)**	32.3 (±3.9)	**24.2 (±7.4)**	25.9 (±3.5)	13.7 (±5.1)	11.8 (±3.1)	**8.6 (±4.7)**	9.3 (±3.0)
Forest	35.9 (±6.5)	35.9 (±6.5)	36.1 (±7.0)	36.1 (±7.0)	30.2 (±7.2)	30.2 (±7.2)	13.1 (±5.2)	13.1 (±5.2)	10.1 (±4.7)	10.1 (±4.7)
Pasture	**30.1 (±8.5)**	32.8 (±4.2)	**30.5 (±8.6)**	32.8 (±4.2)	32.3 (±8.1)	26.3 (±3.8)	21.1 (±5.8)	12.7 (±2.8)	13.3 (±4.1)	9.5 (±2.1)
Planted Forest	**23.8 (±6.0)**	36.6 (±2.5)	**23.9 (±6.1)**	36.6 (±2.5)	**23.5 (±5.6)**	29.5 (±2.4)	16.9 (±4.6)	14.2 (±2.6)	**10.8 (±4.3)**	11.7 (±2.6)
Vineyard	**26.0 (±7.9)**	33.9 (±4.8)	**26.0 (±8.0)**	33.9 (±4.9)	**21.8 (±8.0)**	26.6 (±4.5)	12.0 (±5.5)	11.4 (±3.9)	**7.4 (±4.4)**	8.9 (±3.3)

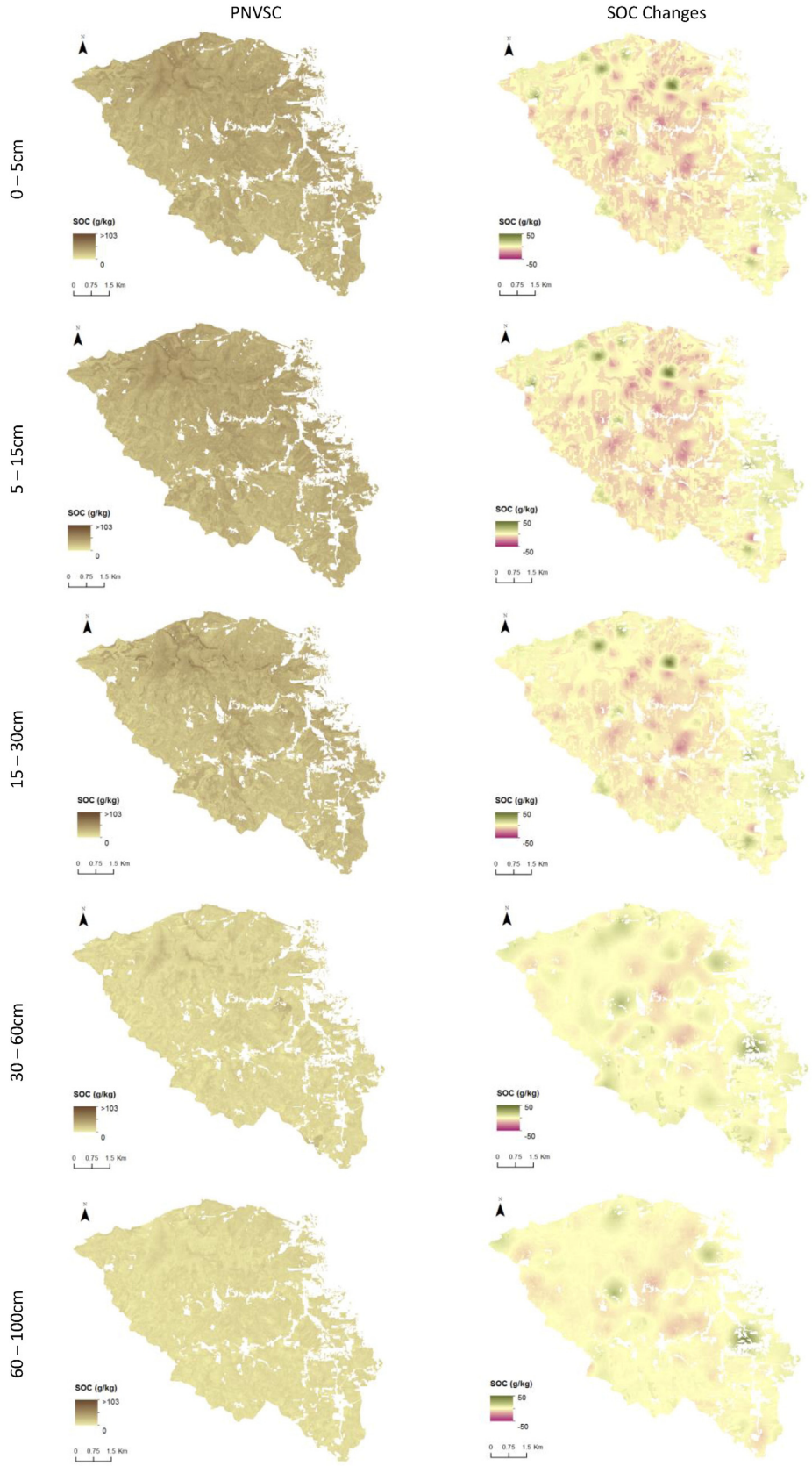

Fig. 11. Maps of Projected Natural Vegetation Soil Carbon (PNVSC) and changes in SOC in Vale dos Vinhedos in Rio Grande do Sul, Brazil.

organic material, which is incorporated into the soil. Aboveground input and relatively low rates of decomposition generally increases topsoil SOC levels compared to grasslands (Don et al., 2011; Guo and Gifford, 2002; Jobbágy and Jackson, 2000). For pasture, deep roots contribute to the accumulation of SOC with depth (Guo and Gifford, 2002).

Table 8
SOC stocks (t/ha) under different land use and in different soils in various parts of the world.

Location	Land use, soil type	Depth	SOC stocks (t C/ha)	Reference
Brazil — Distrito Federal	Tillage — 6 treatments	100 cm	171	Jantalia et al. (2007)
Brazil — Rio Grande do Sul	3 different crop rotations in:			Sisti et al. (2004)
	Zero till	100 cm	175.2	
	Conventional tillage		163.8	
Brazil — Rio Grande do Sul	Rotations with intercropped or cover–crop legumes in:			Boddey et al. (2010)
	Zero till	100 cm	154–172	
	Conventional tillage		132–163	
Brazil — Rio Grande do Sul	Alfisols	30 cm	77	Tornquist et al. (2009a)
	Entisols		66	
	Inceptisols		83	
	Mollisols		76	
	Oxisols		77	
	Ultisols		48	
Brazil	Mixed Ombrophyllous forest	30 cm	61–128	Bernoux et al. (2002)
Brazil — Amazon	Forest on Arenosol	100 cm	40	Batjes and Dijkshoorn (1999)
	Forest on Histosol		724	
Spain — Canalda river basin	Cropland (mainly cereals and potatoes)	100 cm	63	Simó et al. (2014)
	Forest		116	
	Grazing		89	
USA	–	100 cm	345	Wills et al. (2014)
USA	Forest	100 cm	76.8	Bliss et al. (2014)
	Pasture		74.9	
	Crops (82 row crops)		107	
China	Forestland	100 cm	143.3	Yu et al. (2007)
	Grassland		82.4	
	Farmland		92.2	
Rwanda — Rukarara river catchment	Forest	50 cm	295–487	Wasige et al. (2014)
	Agriculture (tea, coffee, maize and banana)		114–169	

Soils under arable crops and vineyard had the lowest SOC concentration and stocks as a result of reduced organic matter input and enhanced decomposition (Elliott, 1986; Sanford, 2014; Schrumpf et al., 2013), but SOC levels could improve with careful soil management (Lal, 2006). Soil erosion may decrease SOC stocks in agricultural systems (Don et al., 2011) whereas leaving the land fallow may increase SOC levels depending on the length of the fallow. Hartemink (1998) found, in Papua New Guinea, that SOC concentration changed from 51 g C/kg to 36 g C/kg after 17 years of sugarcane cultivation.

Planted forests in Vale dos Vinhedos are mostly pinus or eucalyptus, and the soils generally had a low SOC concentration and SOC stocks. It is known that coniferous and broadleaf trees can have different carbon accumulation (Guo and Gifford, 2002) but we were not able to distinguish these forest types. Planted broadleaf trees accumulate SOC levels comparable to natural forests. Soil C stocks under plantation forest could be restored to the original level under native forest, but it may requires several decades (Guo and Gifford, 2002; O'Brien and Jastrow, 2013). As planted forests are harvested there may be considerable soil erosion and loss of topsoil carbon (Hartemink, 2003).

The SOC concentration and stocks differed by soil order. Until 30 cm soil depth, Entisols have a higher SOC concentration but with depth Oxisols have the highest SOC concentration. Most Entisols (58%) are under forest which explains some of the higher SOC concentrations. Oxisols are deeper soils and have possibility of long-term accumulation of SOC with depth. Many of the Oxisols are under pasture (16%), whereas other soil orders have less than 3% of their area under pasture. Pasture has generally higher SOC accumulation with depth. Alfisols are mostly under vineyard which can explain their lower SOC levels. About two-third of the Mollisols are under forest, accumulating more SOC in upper layers. Most of the Inceptisols are under forest (39%) and vineyard (35%).

SOC stocks were calculated and corrected based on equivalent soil mass (Gifford and Roderick, 2003; Lee et al., 2009; Ellert and Bettany, 1995). We found corrected SOC stocks varying from 104 t C/ha in vineyards in Alfisols to 280 t C/ha in pasture areas in Oxisols, with an average of 161 t C/ha. Results of SOC stocks for 100 cm depth (Table 6, Fig. 7) are comparable to other studies (Table 8). This can be attributed to the relatively high SOC concentrations. About 16% of the SOC concentration values between 60 and 100 cm depth exceeded 10 g C/kg, and considering 40 cm thickness it explains the relative high SOC stocks with depths. Environmental conditions in the study area favor SOC accumulation, due the high precipitation and relatively low temperature. SOC stocks average for soils under arable crops is 163 t C/ha, for fallow is 175 t C/ha, for pasture is 205 t C/ha, vineyard is 150 t C/ha, for planted forest is 149 t C/ha and 184 t C/ha for soils under forest. Other studies in Brazil found similar values such the studies by Boddey et al. (2010), Sisti et al. (2004) and Jantalia et al. (2007) (Table 8).

Tornquist et al. (2009a) found in Rio Grande do Sul State, for SOC stocks to 30 cm soil depth of non-sandy and non-wet soils, mean values of 77 t C/ha for Alfisols, 66 t C/ha for Entisols, 83 t C/ha for Inceptisols, 76 t C/ha for Mollisols, 77 t C/ha for Oxisols and 48 t C/ha for Ultisols. These stocks are comparable to the current study in Vale dos Vinhedos, based on equivalent soil mass, of 57 t C/ha for Alfisols, 85 t C/ha for Entisols, 76 t C/ha for Inceptisols, 60 t C/ha for Mollisols, 106 t C/ha for Oxisols and 67 t C/ha for Ultisols. Bernoux et al. (2002) found for non-sandy or non-wet soils, in areas with mixed forest, SOC stocks (0–30 cm) between 61 and 128 t C/ha. These values are comparable to 84 t C/ha found in forest areas in Vale dos Vinhedos at the same depth based on the equivalent soil mass. Wasige et al. (2014), studying SOC in Rwanda until 50 cm depth, found under forest, stocks ranged 295 t C/ha in Cambisols to 487 t C/ha in Histosols. These values were not corrected by mass and are higher than the 115 t C/ha found in Vale dos Vinhedos (Table 6), for forest until 60 cm depth, corrected by mass. For agriculture areas (main crops are tea, coffee, maize and banana), the values were between 114 t C/ha in Acrisols (Ultisols) and 169 t C/ha in Ferralsols (Oxisols). These SOC stocks are similar to found in arable crops (126.3 t C/ha) and vineyard (115 t C/ha) areas in our study up to 60 cm soil depth.

4.4. Uncertainty and probability maps

It was found that 88% of validation values are within the prediction intervals. Malone et al. (2011) found similar result using an empirical uncertainty method based in distribution of prediction errors. However, for depth with higher spatial covariance of residuals (30–60 cm and

60–100 cm) more than 90% of the values were within the prediction intervals. Our results suggest that the methodology adopted to calculate uncertainty depends of the spatial covariance of the residuals. The limited accuracy may be related to variation in environmental conditions between the training and validation data, lower spatial relation found in the most of interval depths, and errors in measures of the training or validation samples.

The SOC stocks probability maps (Fig. 10) reflect SOC stocks exceeding 184 t C/ha. Such areas are found in valley bottoms due the sediment accumulation and reduced drainage, and in Entisols, Mollisols under forest because of higher production of organic material and lower rates of decomposition. The low probability values are mostly in soils under vineyard or arable crops (mainly Inceptisols and Ultisols). The maps shows that only about 13% of the area has 80% of probability for exceeding the 184 t C/ha. These areas may have the same or more SOC than the soils under original land use. The 20% probability map shows that non-colored areas have 80% of probability to be able to stock more SOC. About 42% of soils of study area (3374 ha) could sequester more carbon if occupied by natural forest.

4.5. Soil C changes

The PNVSC analysis showed that the topsoils could accumulate more SOC if they were under forest (Table 7) because of increased organic material addition and reduced decomposition. Below 15 cm depth, soils under pasture have a higher capacity to accumulate SOC which is commonly found (Guo and Gifford, 2002; Lacoste et al., 2014; Nieder and Benbi, 2008). At interval depth 30–60 cm, regardless of soil type or land use, the soil accumulates more carbon than if the soil was under forest. A possible explanation is that there is storage in carbon in that depth after carbon being translocated from upper layers.

5. Conclusions

From this research the following can be concluded:

- Up to 30 cm soil depth the primary covariates for prediction SOC concentration were Entisols, *X* coordinate, DEM and Aspect.
- With depth, the primary covariates for prediction SOC concentration were Overland Flow Distance, Aspect, Soil Order, *Y* coordinate.
- For the prediction of the soil depth, the primary covariates were Soil Order and Valley Depth.
- Forest accumulates more carbon in upper layers and pasture accumulates more carbon with depth.
- Oxisols and Entisols accumulate larger contents of SOC. Lower values for SOC were found in Alfisols, Ultisols, arable crops, vineyard and planted forest.
- The SOC stocks (down to 100 cm) were on average 166 t C/ha but varied between 107 t C/ha in vineyards on Alfisols, and 324 t C/ha in fallow areas on Oxisols.
- The PNVSC analysis showed that carbon was lost when land use changes from natural environment, reducing the potential of carbon sequestration.

Acknowledgments

We are especially grateful to Carlos Alberto Flores, Reinaldo Oscar Pötter, Eliana Casco Sarmento, Eliseu José Weber and Heinrich Hasenack, for the soil survey in Vale dos Vinhedos and for making the data available. The first author was supported by the CAPES Foundation, Ministry of Education of Brazil (Process BEX 3095/14-2). We are grateful to Prof. Budiman Minansny of the University of Sydney who made useful comments on the draft of this paper, and to two anonymous reviewers for their suggestions that improved this paper.

References

Adhikari, K., Hartemink, A.E., 2015. Digital mapping of topsoil carbon content and changes in the Driftless Area of Wisconsin, USA. Soil Sci. Soc. Am. J. 79, 155–164. http://dx.doi.org/10.2136/sssaj2014.09.0392.

Adhikari, K., Hartemink, A.E., Minasny, B., Bou Kheir, R., Greve, M.B., Greve, M.H., 2014. Digital mapping of soil organic carbon contents and stocks in Denmark. PLoS ONE 9, e105519. http://dx.doi.org/10.1371/journal.pone.0105519.

Angers, D.A., Eriksen-Hamel, N.S., 2008. Full-inversion tillage and organic carbon distribution in soil profiles: a meta-analysis. Soil Sci. Soc. Am. J. 72, 1370–1374.

Anjos, L.H.C., Jacomine, P.K., dos Santos, H.G., de Oliveira, V.A., de Oliveria, J.B., 2012. Sistema Brasileiro de Classificação de Solos. In: Ker, J.C., Curi, N., Schaefer, C.E.G., Vidal-Torrado, P. (Eds.), Pedologia; Fundamentos. SBCS, Viçosa, MG.

Arrouays, D., Grundy, M.G., Hartemink, A.E., Hempel, J.W., Heuvelink, G.B.M., Hong, S.Y., Lagacherie, P., Lelyk, G., McBratney, A.B., McKenzie, N.J., Mendonca-Santos, M.D.L., Minasny, B., Montanarella, L., Odeh, I.O.A., Sanchez, P.A., Thompson, J.A., Zhang, G.L., 2014. GlobalSoilMap: toward a fine-resolution global grid of soil properties. Adv. Agron. 125, 93–134.

Batjes, N.H., Dijkshoorn, J.A., 1999. Carbon and nitrogen stocks in the soils of the Amazon Region. Geoderma 89, 273–286. http://dx.doi.org/10.1016/S0016-7061(98)00086-X.

Benites, V.M., Machado, P.L.O.A., Fidalgo, E.C.C., Coelho, M.R., Madari, B.E., 2007. Pedotransfer functions for estimating soil bulk density from existing soil survey reports in Brazil. Geoderma 139, 90–97. http://dx.doi.org/10.1016/j.geoderma.2007.01.005.

Berhongaray, G., Alvarez, R., De Paepe, J., Caride, C., Cantet, R., 2013. Land use effects on soil carbon in the Argentine Pampas. Geoderma 192, 97–110. http://dx.doi.org/10.1016/j.geoderma.2012.07.016.

Bernoux, M., Carvalho, M. da C.S., Volkoff, B., Cerri, C.C., 2002. Brazil's soil carbon stocks. Soil Sci. Soc. Am. J. 66, 888–896.

Bliss, N.B., Waltman, S.W., West, L.T., Neale, A., Mehaffey, M., 2014. Distribution of soil organic carbon in the conterminous United States. In: Hartemink, A.E., McSweeney, K. (Eds.), Soil CarbonProgress in Soil Science. Springer, Dordrecht, pp. 85–93.

Boddey, R.M., Jantalia, C.P., Conceição, P.C., Zanatta, J.A., Bayer, C., Mielniczuk, J., Dieckow, J., Dos Santos, H.P., Denardin, J.E., Aita, C., Giacomini, S.J., Alves, B.J.r., Urquiaga, S., 2010. Carbon accumulation at depth in Ferralsols under zero-till subtropical agriculture. Glob. Chang. Biol. 16, 784–795. http://dx.doi.org/10.1111/j.1365-2486.2009.02020.x.

Breiman, L., 2001. Random forests. Mach. Learn. 45, 5–32.

Brogniez, D., Ballabio, C., van Wesemael, B., Jones, R.A., Stevens, A., Montanarella, L., 2014. Topsoil organic carbon map of Europe. In: Hartemink, A.E., McSweeney, K. (Eds.), Soil CarbonProgress in Soil Science. Springer, Dordrecht, pp. 393–405.

Cerri, C.C., Andreux, F., 1990. Changes in organic carbon content in Oxisols cultivated with sugar cane and pasture, based on ^{13}C natural abundance measurement. Transactions 14th International Congress of Soil Science, Kyoto, Japan, August 1990 vol. IV, pp. 98–103.

Cerri, C.E.P., Easter, M., Paustian, K., Killian, K., Coleman, K., Bernoux, M., Falloon, P., Powlson, D.S., Batjes, N.H., Milne, E., Cerri, C.C., 2007. Predicted soil organic carbon stocks and changes in the Brazilian Amazon between 2000 and 2030. Agric. Ecosyst. Environ. 122, 58–72. http://dx.doi.org/10.1016/j.agee.2007.01.008.

Cheng, X.F., Shi, X.Z., Yu, D.S., Pan, X.Z., Wang, H.J., Sun, W.X., 2004. Using GIS spatial distribution to predict soil organic carbon in subtropical China. Pedosphere 14, 425–431.

Collard, F., Saby, N., de Forges, A.R., Lehmann, S., Paroissien, J.-B., Arrouays, D., 2014. Spatial prediction of soil organic carbon at different depths using digital soil mapping. In: Arrouays, D., McKenzie, N., Hempel, J., de Forges, A.C. Richer, McBratney, A. (Eds.), GlobalSoilMap — Basis of the Global Spatial Information Systems. CRC Press, pp. 181–184.

Conant, R., Puastian, K., Elliot, E., 2001. Grassland management and conversion into grassland: effects on soil carbon. Ecol. Appl. 11, 343–355.

de Souza, E., Hengl, T., Kempen, B., Heuvelink, G., Filho, E.F., Schaefer, C., 2014. Comparing spatial prediction methods for soil property mapping in Brazil. In: Arrouays, D., McKenzie, N., Hempel, J., de Forges, A.C. Richer, McBratney, A. (Eds.), GlobalSoilMap — Basis of the Global Spatial Information Systems. CRC Press, pp. 267–271.

Dietrich, H., Böhner, J., 2008. Cold air production and flow in a low mountain range landscape in Hessia (Germany). Hambg. Beitr. Zur Phys. Geogr. Landschaftsökologie.

Don, A., Schumacher, J., Freibauer, A., 2011. Impact of tropical land-use change on soil organic carbon stocks — a meta-analysis. Glob. Chang. Biol. 17, 1658–1670. http://dx.doi.org/10.1111/j.1365-2486.2010.02336.x.

Ellert, B.H., Bettany, J.R., 1995. Calculation of organic matter and nutrients stored in soils under contrasting management regimes. Can. J. Soil Sci. 75, 529–538. http://dx.doi.org/10.4141/cjss95-075.

Elliott, E.T., 1986. Aggregate structure and carbon, nitrogen, and phosphorus in native and cultivated soils. Soil Sci. Soc. Am. J. 50, 627–633.

EMBRAPA, 2008. Normal Climatológica: Estação Agroclimática da Embrapa Uva e Vinho, Bento Gonçalves, RS. Período de 1961 a 1990. http://www.cnpuv.embrapa.br/.

Flores, C.A., Pötter, R.O., Sarmento, E.C., Weber, E.J., Hasenack, H., 2012. Os Solos do Vale dos Vinhedos. EMBRAPA, Brasília, DF. Brazil.

Forges, A.C., Martin, M.P., Saby, N.P.A., Arrouays, D., Martelet, G., Tourlière, B., 2014. A preliminary analysis of topsoil organic carbon contents and stocks spatial distribution in a region of France (Région Centre). In: Arrouays, D., McKenzie, N., Hempel, J., de

Forges, A.C. Richer, McBratney, A. (Eds.), GlobalSoilMap — Basis of the Global Spatial Information Systems. CRC Press, pp. 197–200.
Giasson, E., Clarke, R.T., Inda-Junior, A.V., Merten, G.H., Tornquist, C.G., 2006. Digital soil mapping using multiple logistic regression on terrain parameters in southern Brazil. Sci. Agric. 63.
Gifford, R.M., Roderick, M.L., 2003. Soil carbon stocks and bulk density: spatial or cumulative mass coordinates as a basis of expression? Glob. Chang. Biol. 9, 1507–1514.
Guo, L.B., Gifford, R.M., 2002. Soil carbon stocks and land use change: a meta analysis. Glob. Chang. Biol. 8, 345–360. http://dx.doi.org/10.1046/j.1354-1013.2002.00486.x.
Hair, J.F., Black, W.C., Babin, B.J., Anderson, R.E., 2009. Multivariate Data Analysis. 7th ed. Prentice Hall.
Hartemink, A.E., 1998. Soil chemical and physical properties as indicators of sustainable land management under sugar cane in Papua New Guinea. Geoderma 85, 283–306. http://dx.doi.org/10.1016/S0016-7061(98)00048-2.
Hartemink, A.E., 2003. Soil Fertility Decline in the Tropics: With Case Studies on Plantations. CABI, Wallingford, UK.
Hartemink, A.E., McSweeney, K. (Eds.), 2014. Soil Carbon. Springer, Dordrecht.
IBGE, 1986. Folha SH.22 Porto Alegre e parte das Folhas SH.21 Uruguaiana e SI.22 Lagoa Mirim. Levantamento de Recursos Naturais. IBGE, Rio de Janeiro.
Jantalia, C.P., Resck, D.V.S., Alves, B.J.R., Zotarelli, L., Urquiaga, S., Boddey, R.M., 2007. Tillage effect on C stocks of a clayey Oxisol under a soybean-based crop rotation in the Brazilian Cerrado region. Soil Tillage Res. 95, 97–109. http://dx.doi.org/10.1016/j.still.2006.11.005.
Jobbágy, E.G., Jackson, R.B., 2000. The vertical distribution of soil organic carbon and its relation to climate and vegetation. Ecol. Appl. 10, 423–436.
Kirsten, M., Kaaya, A., Klinger, T., Feger, K.-H., 2015. Stocks of soil organic carbon in forest ecosystems of the Eastern Usambara Mountains, Tanzania. Catena http://dx.doi.org/10.1016/j.catena.2014.12.027.
Lacoste, M., Minasny, B., McBratney, A., Michot, D., Viaud, V., Walter, C., 2014. High resolution 3D mapping of soil organic carbon in a heterogeneous agricultural landscape. Geoderma 213, 296–311. http://dx.doi.org/10.1016/j.geoderma.2013.07.002.
Lal, R., 2005. Forest soils and carbon sequestration. For. Ecol. Manag. 220, 242–258. http://dx.doi.org/10.1016/j.foreco.2005.08.015.
Lal, R., 2006. Enhancing crop yields in the developing countries through restoration of the soil organic carbon pool in agricultural lands. Land Degrad. Dev. 17, 197–209. http://dx.doi.org/10.1002/ldr.696.
Lee, J., Hopmans, J.W., Rolston, D.E., Baer, S.G., Six, J., 2009. Determining soil carbon stock changes: simple bulk density corrections fail. Agric. Ecosyst. Environ. 134, 251–256. http://dx.doi.org/10.1016/j.agee.2009.07.006.
Libohova, Z., Stott, D.E., Owens, P.R., Winzeler, H.E., Wills, S., 2014. Mineralizable soil organic carbon dynamics in corn–soybean rotations in glaciated derived landscapes of Northern Indiana. In: Hartemink, A.E., McSweeney, K. (Eds.), Soil Carbon. Springer, Dordrecht, pp. 259–269.
MacMillan, R.A., 2003. LandMapR Software Toolkit — C++ Version. Users manual. LandMapper Environmental Solutions Inc., Edmonton.
Malone, B., 2013. Use R for Digital Soil Mapping. Univ. Syd.
Malone, B.P., McBratney, A.B., Minasny, B., Laslett, G.M., 2009. Mapping continuous depth functions of soil carbon storage and available water capacity. Geoderma 154, 138–152. http://dx.doi.org/10.1016/j.geoderma.2009.10.007.
Malone, B.P., McBratney, A.B., Minasny, B., 2011. Empirical estimates of uncertainty for mapping continuous depth functions of soil attributes. Geoderma 160, 614–626.
Mendonça-Santos, M.L., Santos, H.G., 2007. The state of the art of Brazilian soil mapping and prospects for digital soil mapping. In: Lagacherie, P., McBratney, A.B., Voltz, M. (Eds.), Digital Soil Mapping: An Introductory Perspective. Elsevier, Amsterdam.
Mendonça-Santos, M.L., Dart, R.O., Santos, H.G., Coelho, M.R., Berbara, R.L.L., Lumbreras, J.F., 2010. Digital soil mapping of topsoil organic carbon content of Rio de Janeiro State, Brazil. In: Boettinger, D.J.L., Howell, D.W., Moore, A.C., Hartemink, P.D.A.E., Kienast-Brown, S. (Eds.), Digital Soil Mapping, Progress in Soil Science. Springer, Netherlands, pp. 255–266.
Minasny, B., McBratney, A.B., 2013. Jenny, PCA and random forests. Pedometron 33, 10–13.
Minasny, B., McBratney, A.B., Malone, B.P., Wheeler, I., 2013. Digital mapping of soil carbon. Adv. Agron. 118, 1–47. http://dx.doi.org/10.1016/b978-0-12-405942-9.00001-3.
Nieder, R., Benbi, D.K., 2008. Carbon and Nitrogen in the Terrestrial Environment. Springer, Dordrecht.
O'Brien, S.L., Jastrow, J.D., 2013. Physical and chemical protection in hierarchical soil aggregates regulates soil carbon and nitrogen recovery in restored perennial grasslands. Soil Biol. Biochem. 61, 1–13. http://dx.doi.org/10.1016/j.soilbio.2013.01.031.
Padarian, J., Pérez-Quezada, J., Seguel, O., 2012. Modelling the distribution of organic carbon in the soils of Chile. In: Minasny, B., Malone, B.P., McBratney, A.B. (Eds.), Digital Soil Assessments and Beyond. CRC Press, pp. 329–333.
Quinlan, J.R., 1992. Leaning with continuous classes. In: Adams, A., Sterling, L. (Eds.), Proceedings of AI92, 5th Australian Conference on Artificial Intelligence. World Scientific, Singapore, pp. 343–348.
Ross, C.W., Grunwald, S., Myers, D.B., 2013. Spatiotemporal modeling of soil organic carbon stocks across a subtropical region. Sci. Total Environ. 461–462, 149–157. http://dx.doi.org/10.1016/j.scitotenv.2013.04.070.
Rumpel, C., Kögel-Knabner, I., 2011. Deep soil organic matter—a key but poorly understood component of terrestrial C cycle. Plant Soil 338, 143–158. http://dx.doi.org/10.1007/s11104-010-0391-5.
Sanford, G.R., 2014. Perennial grasslands are essential for long term SOC storage in the Mollisols of the North Central USA. In: Hartemink, A.E., McSweeney, K. (Eds.), Soil Carbon. Springer, Dordrecht, pp. 281–288.
Santos, H.G., Jacomine, P.K., dos Anjos, L.H.C., de Oliveira, V.A., de Oliveira, J.B., Coelho, M.R., Lumbreras, J.F., Cunha, T.J.F., 2006. Sistema Brasileiro de Classificação de Solos. 2nd ed. Embrapa Solos, Rio de Janeiro.
Schrumpf, M., Kaiser, K., Guggenberger, G., Persson, T., Kögel-Knabner, I., Schulze, E.-D., 2013. Storage and stability of organic carbon in soils as related to depth, occlusion within aggregates, and attachment to minerals. Biogeosciences 10, 1675–1691. http://dx.doi.org/10.5194/bg-10-1675-2013.
Shrestha, D.L., Solomatine, D.P., 2006. Machine learning approaches for estimation of prediction interval for the model output. Neural Netw. 19, 225–235. http://dx.doi.org/10.1016/j.neunet.2006.01.012.
Simó, I., Herrero, C., Boixadera, J., Poch, R., de Forges, A.C. Richer, 2014. Modelling soil organic carbon stocks using a detailed soil map in a Mediterranean mountainous area. In: Arrouays, D., McKenzie, N., Hempel, J., McBratney, A. (Eds.), GlobalSoilMap — Basis of the Global Spatial Information Systems. CRC Press, pp. 421–427.
Sisti, C.P.J., dos Santos, H.P., Kohhann, R., Alves, B.J.R., Urquiaga, S., Boddey, R.M., 2004. Change in carbon and nitrogen stocks in soil under 13 years of conventional or zero tillage in southern Brazil. Soil Tillage Res. 76, 39–58. http://dx.doi.org/10.1016/j.still.2003.08.007.
Solomatine, D.P., Shrestha, D.L., 2009. A novel method to estimate model uncertainty using machine learning techniques: novel method to estimate uncertainty. Water Resour. Res. 45. http://dx.doi.org/10.1029/2008WR006839.
Thompson, J.A., Kolka, R.K., 2005. Soil carbon storage estimation in a forested watershed using quantitative soil-landscape modeling. Soil Sci. Soc. Am. J. 69, 1086–1093.
Tornquist, C.G., Giasson, E., Mielniczuk, J., Cerri, C.E.P., Bernoux, M., 2009a. Soil organic carbon stocks of Rio Grande do Sul, Brazil. Soil Sci. Soc. Am. J. 73, 975. http://dx.doi.org/10.2136/sssaj2008.0112.
Tornquist, C.G., Mielniczuk, J., Cerri, C.E.P., 2009b. Modeling soil organic carbon dynamics in Oxisols of Ibirubá (Brazil) with the Century Model. Soil Tillage Res. 105, 33–43. http://dx.doi.org/10.1016/j.still.2009.05.005.
Tranter, G., Minasny, B., Mcbratney, A.B., Murphy, B., Mckenzie, N.J., Grundy, M., Brough, D., 2007. Building and testing conceptual and empirical models for predicting soil bulk density. Soil Use Manag. 23, 437–443. http://dx.doi.org/10.1111/j.1475-2743.2007.00092.x.
Vasques, G.M., Grunwald, S., Comerford, N.B., Sickman, J.O., 2010. Regional modelling of soil carbon at multiple depths within a subtropical watershed. Geoderma 156, 326–336. http://dx.doi.org/10.1016/j.geoderma.2010.03.002.
Waring, C., Stockman, U., Malone, B., Whelan, B., McBratney, A.B., 2014. Is percent "Projected Natural Vegetation Soil Carbon" a useful indicator of soil condition? In: Hartemink, A., McSweeney, K. (Eds.), Soil Carbon. Springer, pp. 219–227
Wasige, J.E., Groen, T.A.E., Rwamukwaya, B.M., Tumwesigye, W., Smaling, E.M.A., Jetten, V., 2014. Contemporary land use/land cover types determine soil organic carbon stocks in south-west Rwanda. Nutr. Cycl. Agroecosyst. 100, 19–33. http://dx.doi.org/10.1007/s10705-014-9623-z.
Wiesmeier, M., Barthold, F., Spörlein, P., Geuß, U., Hangen, E., Reischl, A., Schilling, B., Angst, G., von Lützow, M., Kögel-Knabner, I., 2014. Estimation of total organic carbon storage and its driving factors in soils of Bavaria (southeast Germany). Geoderma Reg. 1, 67–78. http://dx.doi.org/10.1016/j.geodrs.2014.09.001.
Wills, S., Loecke, T., Sequeira, C., Teachman, G., Grunwald, S., West, L.T., 2014. Overview of the U.S. rapid carbon assessment project: sampling design, initial summary and uncertainty estimates. In: Hartemink, A.E., McSweeney, K. (Eds.), Soil Carbon. Springer International Publishing, pp. 95–104.
Yu, D.S., Shi, X.Z., Wang, H.J., Sun, W.X., Chen, J.M., Liu, Q.H., Zhao, Y.C., 2007. Regional patterns of soil organic carbon stocks in China. J. Environ. Manag. 85, 680–689. http://dx.doi.org/10.1016/j.jenvman.2006.09.020.
Zhang, P., Shao, M., 2014. Spatial variability and stocks of soil organic carbon in the Gobi desert of Northwestern China. PLoS ONE 9, e93584.